Structural and Multidisciplinary Optimization manuscript No.
(will be inserted by the editor)

ESLA: a new Surrogate-Assisted Single-Loop Reliability-Based Design Optimization technique

Jolan Wauters · Ivo Couckuyt · Joris Degroote

Received: date / Accepted: date

Abstract In this paper, we address the formulation of a novel scheme for reliability-based design optimization, in which the design optimization problem is characterized by constraints that must be met with a certain probability. Assessment of the aforementioned is typically referred to as reliability analysis. Conventional methods rely on sampling approaches or by reformulating the problem as a two-level optimization that requires gradient or Hessian information of the constraints to obtain a trustworthy solution. However, the computational cost of such methods makes them often impractical. To overcome the aforementioned, a surrogate-assisted asymptotic reliability analysis (SARA) is presented that makes use of surrogate-derived gradient and Hessian information. The sub-optimization problem is reformulated as a set of constraints using the Karush-Kuhn-Tucker conditions and fitted in an efficient global optimization-like setting through the formulation of the reliability-based expected improvement (RBEI), obtaining the novel efficient single-loop approach (ESLA). The method is tested on a series of test cases which prove the effectiveness of the novel scheme.

Keywords Surrogate Modeling · Kriging · Reliability-Based Design Optimization · Reliability Analysis · Karush-Kuhn-Tucker · Uncertainty Quantification

Conducted as part of the SBO research project 140068 EUFORIA (Efficient Uncertainty quantification For Optimization in Robust design of Industrial Applications) under the financial support of the IWT, the Flemish agency of Innovation through Science and Technology.

Jolan Wauters, Joris Degroote
Ghent University
Department of Electromechanical, Systems and Metals Engineering (ESME)
Sint-Pietersnieuwstraat 41, 9000 Gent, Belgium
E-mail: {jolan.wauters, joris.degroote}@ugent.be

Ivo Couckuyt
Ghent University
Department of Information Technology (INTEC)
iGent, Technologiepark-Zwijnaarde 15, 9052 Gent, Belgium
E-mail: ivo.couckuyt@ugent.be

1 Introduction

In this paper we examine surrogate-assisted *reliability-based design optimization* (RBDO). NASA defines a *reliability-based design* problem as a problem that *"seeks a design that has a probability of failure that is less than some acceptable (invariably small) value"* [80]. *Reliability analysis* (RA) corresponds with the assessment of probability of meeting a constraint g (with $g \leq 0$ denoting failure). To state this more broadly, RA corresponds to the process of determining the probability of failure P_f of a system which depends on a random (aleatoric or irreducible) input $\mathfrak{u}$[1]. This can be understood as calculating the area under the (joint) probability distribution $f_{\mathfrak{u}}(\mathfrak{u})$ cut-off by the *limit-state surface* $\mathscr{F} = \{\mathfrak{u} \in \mathfrak{U} : g(\mathfrak{u}) = 0\}$, the boundary determining failure[2], so over the *failure domain* $\mathbb{F} = \{\mathfrak{u} \in \mathfrak{U} : g(\mathfrak{u}) \leq 0\}$[3][4]. The probability of failure can formally be written as

$$P_f = \mathbb{P}[g(\mathfrak{u}) \leq 0] = \int_{\mathbb{F}} f_{\mathfrak{u}}(\mathfrak{u}) d\mathfrak{u} \tag{1}$$

Broadly speaking the field of reliability analysis can be divided in two categories based on the manner by which the multivariate integral is evaluated: sampling based methods and *most probable point* (MPP) based approaches[5]. Of the sampling based approaches, Monte Carlo sampling is undoubtedly the most well known. However, the slow convergence rate, especially on the estimation of tail probability, has lead to the development of a number of improvements such as variance reducing methods (e.g. importance sampling [61, 25, 75] and subset sampling [4, 44]) and inference methods, in which a distribution is fitted based on a sample set. A recent improvement on the latter method is the inference on the tail distribution [10, 55, 64]. A more complete and in-depth overview is given in Lemaire [42].

Sampling methods require hundreds to thousands of samples to obtain a trustworthy estimate, even using the improved sampling techniques discussed above. This has lead to the development of MPP-based approaches. Originally these were developed in the standard normal space, but they have since been extended to non-normal spaces. Probable point approaches rely on the approximation of the limit surface in the point with the greatest probability of occurrence (and the point closest to the origin in the standard normal space). This, along with the

[1] The *Fraktur* font is used to denote aleatory uncertainties.

[2] In the field of Economics this is sometimes called a *Black Swan* in reference to the work of Nassim Nicholas Taleb (2007). However, paradoxically Taleb states that we are unable to recognize the black swans and should therefore incorporate a level of robustness to account for unpredictable events.

[3] An imprecise probabilistic approach to reliability analysis using p-boxes [49] and a non-probabilistic approach to reliability analysis using for example fuzzy logic [47], evidence theory [11, 34, 81], possibility theory, interval analysis [73] and convex modeling [82, 71] can alternatively be used when insufficient information is available to make a trustworthy estimate of the pdf of the input.

[4] In this work time-invariant, component-level reliability analysis is examined. For the sake of compactness RA will be used for the remainder of the paper. Recent studies towards time-variant RA are amongst other found in [32, 45, 63, 72, 70] and towards system-level RA in [79, 7].

[5] Not all existing methods, such as Haldar & Mahadevan's *mean value first-order second-moment* (MVFOSM) method [28], can be straightforwardly be categorized. Alternatively, one could categorize the methods more broadly as single-point approaches.

property of the standard normal space that probabilities decay exponentially with the square of the distance from the origin, lead to fairly accurate estimation of the probability of failure. This can be understood from the observation that the majority of the information on the estimation of reliability is contained in the region around the MPP where the estimation of the limit-surface is most accurate. The two most well known MPP-based approaches are the *first order reliability methods* (FORM) and *second order reliability methods* (SORM), which differ on the order of the hyperplane with which the limit surface is approximated: the former first and the latter second order. However, since SORM requires Hessian information in the MPP, its applicability in industrial cases is limited. An overview of the current state of the aforementioned methods can be found in [59].

The choice between a sampling approach and a MPP-approach is typically presented as the choice between an accurate but unaffordable method and an affordable but inaccurate method. Surrogate modeling has as yet only been examined for the solution to the former, where the often expensive to evaluate model is replaced by a cheap one, but where the accuracy of the reliability analysis is now determined by the accuracy of the surrogate model. A Kriging-based RA is amongst other examined by Bichon through his *efficient global reliability analysis* (EGRA) [6] and Dubourg through meta-model-based importance sampling approach [19, 20]. Arsenyev examined an efficient bridge between the two approaches by applying importance sampling to the MPP obtained through Kriging in an EGO-like manner [3]. An overview of surrogate-aided RA methods is found in [66, 54]. Conventionally, surrogate-based RA methods replace the expensive to evaluate model by a cheaper one, but keep considering it as a black-box. More recent work takes the model-uncertainty of the surrogate into account during its updating, leading to so called *Active Learning Kriging* (ALK) and *Adaptive Kriging* (AK) [21, 33, 78, 74, 79, 48]. In this paper, the analytical formulation of the surrogate is used to perform a SORM-like RA without the need to calculate the first and second derivatives and without the need to sample the surrogate to obtain an estimate of the probability of failure, as such making it especially interesting from an industrial point of view.

The development of a surrogate-assisted reliability-based design optimization framework is presented in a sequence of steps: in §2 of this paper, we present the concept of Kriging and its predictor along with an analytical formulation of the first derivative. We extend on this through the formulation of the second derivative along with its corresponding mean square error, the first contribution of this work. Furthermore, the *efficient global optimization* (EGO) framework, which incorporates the Kriging model in an optimization scheme through the concept of Expected Improvement, is presented. In §3 we present the concepts of asymptotic reliability analysis in the standard normal space and its integration in a surrogate-assisted environment leading to *surrogate-assisted asymptotic reliability analysis* (SARA), the second contribution of this work. In §4 the single-loop reliability-based design optimization problem is presented and in §5 fitted in an EGO-like setting through the introduction of the *reliability-based expected improvement* (RBEI) obtaining the *efficient single-loop approach* (ESLA) scheme, the third contribution of this work. In §6 the framework is tested on a number of analytical test functions characterized by real life difficulties.

2 Efficient Global Optimization

Kriging, or Gaussian process interpolation as it is more commonly known in the fields of statistics and machine learning, is an effective approach to tackle problems that are subjected to a limited number of objective function evaluations, for example due to the prohibitive cost of the experiments or evaluation of the numerical model. The method can be understood as a kernel method in which a prior probability distribution over functions is defined. By means of Bayes' theorem, a posterior probability distribution function over functions can be obtained that passes through a set of evaluated points. These points are typically selected through a well-posed *design of experiments* (DoE), whose objective it is to infer as much information as possible from the objective space. The resulting model can be seen a Gaussian process with mean trend function: $\mathcal{Y}(\mathbf{x}) = \boldsymbol{f}(\mathbf{x})^T\boldsymbol{\beta} + \mathcal{Z}(\mathbf{x})$ with $\boldsymbol{f}(\mathbf{x}) = [f_i(\mathbf{x}), i = 1, ..., M]$ the vector of basis functions, $\boldsymbol{\beta}$ the vector of coefficients and $\mathcal{Z}(\mathbf{x})$ a Gaussian process $\mathcal{GP}(0, \psi(\mathbf{x}_i, \mathbf{x}_j))$, with zero mean and fully described by the covariance function $\psi(\cdot, \cdot)$. With $\mathbf{x}_i$ we refer to the i^{th} sample $(i = 1, ..., N)$ and with $\mathbf{x}^{(i)}$ we refer to the i^{th} component $(i = 1, ..., D_{\mathfrak{x}})$. In this work the epistemic uncertainty corresponds to reducible uncertainty related to the Kriging model and is denoted using a calligraphic font $(\mathcal{Y})$.

The trend function is typically the solution of a regression problem and the Gaussian process captures the variation on this trend to exactly interpolate the evaluated data. To obtain the latter, the hyperparameters that fully define the Gaussian process, corresponding to the parameters of the covariance function, are determined. In the machine learning community this is typically referred to as training the machine. We do this by maximizing the likelihood $\boldsymbol{L}$ that the aforementioned surrogate can reproduce the evaluated data. In practice, the concentrated log-likelihood function is maximized. The construction of the Kriging model is performed using an open-source toolbox ooDACE (*object-orientated Design and Analysis of Computer Experiments*) [17] using a multi-start SQP methodology.

The prediction of an unsampled location $\mathbf{x}$, the *Best Linear Unbiased Prediction* (BLUP), and the variance on that prediction, a measure of epistemic uncertainty, the *Mean Square Predictive Error* (MSPE) are respectively given by

$$\mathbb{E}[\mathcal{Y}(\mathbf{x})] \equiv \mathrm{Y}(\mathbf{x}) = \boldsymbol{f}(\mathbf{x})^T\boldsymbol{\beta} + \boldsymbol{\psi}(\mathbf{x})^T\boldsymbol{\Psi}^{-1}(\mathbf{y} - \mathbf{F}\boldsymbol{\beta}) \tag{2}$$

$$\mathbb{V}[\mathcal{Y}(\mathbf{x})] \equiv s^2(\mathbf{x}) = \sigma^2 \left\{ 1 - \boldsymbol{\psi}(\mathbf{x})^T\boldsymbol{\Psi}^{-1}\boldsymbol{\psi}(\mathbf{x}) + \left[\mathbf{F}^T\boldsymbol{\Psi}^{-1}\boldsymbol{\psi}(\mathbf{x}) - \boldsymbol{f}(\mathbf{x})\right]^T \cdot \left[\mathbf{F}^T\boldsymbol{\Psi}^{-1}\mathbf{F}\right]^{-1} \cdot \left[\mathbf{F}^T\boldsymbol{\Psi}^{-1}\boldsymbol{\psi}(\mathbf{x}) - \boldsymbol{f}(\mathbf{x})\right] \right\} \tag{3}$$

with σ the process variance and $\boldsymbol{F}$ the model matrix $\boldsymbol{F}^{(i,j)} = f_i(\mathbf{x}_j)$ and $\boldsymbol{\Psi}$ the correlation matrix $\boldsymbol{\Psi}^{(i,j)} = \psi(\mathbf{x}_i, \mathbf{x}_j)$, $\boldsymbol{\psi}(\mathbf{x}) = [\psi(\mathbf{x}_1, \mathbf{x}), ..., \psi(\mathbf{x}_N, \mathbf{x})]$ and the *maximum likelihood estimation* (MLE) of the coefficient vector and the process variance defined by $\boldsymbol{\beta} = (\mathbf{F}\boldsymbol{\Psi}^{-1}\mathbf{F})^{-1}\mathbf{F}^T\boldsymbol{\Psi}^{-1}\mathbf{y}$ and $\sigma^2 = \frac{1}{N}(\mathbf{y} - \mathbf{F}\boldsymbol{\beta})^T\boldsymbol{\Psi}^{-1}(\mathbf{y} - \mathbf{F}\boldsymbol{\beta})$.

Furthermore, an analytical formulation of the first derivative of the prediction w.r.t. the design variables [29,30] and the corresponding variance can be formulated. We extend the formulation even further for the second derivatives of the BLUP and the corresponding MSPE of the second derivatives. The derivation of which is given in *Appendix A* by means of the difference quotient approach:

$$\frac{\partial \mathrm{Y}(\mathbf{x})}{\partial \mathbf{x}^{(i)}} = \frac{\partial \boldsymbol{f}(\mathbf{x})}{\partial \mathbf{x}^{(i)}}^T \boldsymbol{\beta} + \frac{\partial \boldsymbol{\psi}(\mathbf{x})}{\partial \mathbf{x}^{(i)}} \boldsymbol{\Psi}^{-1}(\mathbf{y} - \mathbf{F}\boldsymbol{\beta}) \tag{4}$$

$$\begin{aligned} s^2_{\partial \mathrm{Y}/\partial \mathbf{x}^{(i)}}(\mathbf{x}) = \sigma^2 \Bigg\{ & \frac{\partial \boldsymbol{\psi}(\mathbf{x})}{\partial \mathbf{x}^{(i)}}^T \boldsymbol{\Psi}^{-1} \frac{\partial \boldsymbol{\psi}(\mathbf{x})}{\partial \mathbf{x}^{(i)}} + \left[\mathbf{F}^T \boldsymbol{\Psi}^{-1} \frac{\partial \boldsymbol{\psi}(\mathbf{x})}{\partial \mathbf{x}^{(i)}}^T - \frac{\partial \boldsymbol{f}(\mathbf{x})}{\partial \mathbf{x}^{(i)}} \right]^T \\ & \cdot \left[\mathbf{F}^T \boldsymbol{\Psi}^{-1} \mathbf{F} \right]^{-1} \cdot \left[\mathbf{F}^T \boldsymbol{\Psi}^{-1} \frac{\partial \boldsymbol{\psi}(\mathbf{x})}{\partial \mathbf{x}^{(i)}}^T - \frac{\partial \boldsymbol{f}(\mathbf{x})}{\partial \mathbf{x}^{(i)}} \right] \Bigg\} \end{aligned} \tag{5}$$

$$\frac{\partial^2 \mathrm{Y}(\mathbf{x})}{\partial \mathbf{x}^{(i)} \partial \mathbf{x}^{(j)}} = \frac{\partial^2 \boldsymbol{f}(\mathbf{x})}{\partial \mathbf{x}^{(i)} \partial \mathbf{x}^{(j)}}^T \boldsymbol{\beta} + \frac{\partial^2 \boldsymbol{\psi}(\mathbf{x})}{\partial \mathbf{x}^{(i)} \partial \mathbf{x}^{(j)}} \boldsymbol{\Psi}^{-1}(\mathbf{y} - \mathbf{F}\boldsymbol{\beta}) \tag{6}$$

$$\begin{aligned} s^2_{\partial^2 \mathrm{Y}/\partial \mathbf{x}^{(i)} \partial \mathbf{x}^{(j)}}(\mathbf{x}) = \sigma^2 \Bigg\{ & \frac{\partial^2 \boldsymbol{\psi}(\mathbf{x})}{\partial \mathbf{x}^{(i)} \partial \mathbf{x}^{(j)}}^T \boldsymbol{\Psi}^{-1} \frac{\partial^2 \boldsymbol{\psi}(\mathbf{x})}{\partial \mathbf{x}^{(i)} \partial \mathbf{x}^{(j)}} \\ & + \left[\mathbf{F}^T \boldsymbol{\Psi}^{-1} \frac{\partial^2 \boldsymbol{\psi}(\mathbf{x})}{\partial \mathbf{x}^{(i)} \partial \mathbf{x}^{(j)}}^T - \frac{\partial^2 \boldsymbol{f}}{\partial \mathbf{x}^{(i)} \partial \mathbf{x}^{(j)}} \right]^T \cdot \left[\mathbf{F}^T \boldsymbol{\Psi}^{-1} \mathbf{F} \right]^{-1} \\ & \cdot \left[\mathbf{F}^T \boldsymbol{\Psi}^{-1} \frac{\partial^2 \boldsymbol{\psi}(\mathbf{x})}{\partial \mathbf{x}^{(i)} \partial \mathbf{x}^{(j)}}^T - \frac{\partial^2 \boldsymbol{f}(\mathbf{x})}{\partial \mathbf{x}^{(i)} \partial \mathbf{x}^{(j)}} \right] \Bigg\} \end{aligned} \tag{7}$$

The squared exponential covariance function is probably the most often used kernel for Gaussian process regression. Since the function is infinitely differentiable, the interpolated data behaves very smooth. Stein argues that this is nonphysical and proposes the use of the Matérn covariance function instead [65].

$$\psi(\mathbf{x}_i, \mathbf{x}_j) = \frac{2^{1-\nu}}{\Gamma(\nu)} \left(\sqrt{2\nu} \mathcal{L}(\mathbf{x}_i, \mathbf{x}_j) \right)^\nu K_\nu \left(\sqrt{2\nu} \mathcal{L}(\mathbf{x}_i, \mathbf{x}_j) \right) \tag{8}$$

with $\Gamma(\nu)$ the Gamma function, K_ν the modified Bessel function of the second kind and $\mathcal{L}$ the distance function and typically expressed as the *Mahalanobis distance*

$$\begin{aligned} \Gamma(\nu) &= \int_0^\infty t^{\nu-1} \mathrm{e}^{-t} dt, \\ K_\nu(\mathrm{x}) &= \frac{\pi}{2} \frac{I_{-\nu}(\mathrm{x}) - I_\nu(\mathrm{x})}{\sin(\alpha\pi)}, \\ I_\nu(\mathrm{x}) &= \sum_{m=0}^\infty \frac{1}{m! \Gamma(m+\nu+1)} \left(\frac{\mathrm{x}}{2} \right)^{2m+\nu}, \\ \mathcal{L}(\mathbf{x}_i, \mathbf{x}_j) &= \sqrt{\sum_{d=1}^D \theta^{(d)} \left(\mathbf{x}_i^{(d)} - \mathbf{x}_j^{(d)} \right)^2}. \end{aligned}$$

The parameter $\theta^{(d)}$ of the Matérn function is a *width parameter* and ν is a *smoothness parameter*. When $\nu = 1/2 + p$ with $p \in \mathbb{N}$ is used, the function strongly simplifies and is p-times mean square differentiable. Here the case is considered for $p = 2$ resulting in

$$\psi(\mathbf{x}_i, \mathbf{x}_j) = \left(1 + \sqrt{5}\mathcal{L}(\mathbf{x}_i, \mathbf{x}_j) + \frac{5}{3}\mathcal{L}(\mathbf{x}_i, \mathbf{x}_j)^2\right) \exp\left(-\sqrt{5}\mathcal{L}(\mathbf{x}_i, \mathbf{x}_j)\right) \tag{9}$$

The first derivative $\psi'(\mathbf{x}_i, \mathbf{x}_j) = \partial\psi(\mathbf{x}_i, \mathbf{x}_j)/\partial\mathbf{x}_i$ and second derivative $\psi''(\mathbf{x}_i, \mathbf{x}_j) = \partial^2\psi(\mathbf{x}_i, \mathbf{x}_j)/\partial\mathbf{x}_i\partial\mathbf{x}_i$ can be derived using the chain rule with the former being a $D_\mathbf{x} \times 1$ vector and the latter a $D_\mathbf{x} \times D_\mathbf{x}$ matrix of which respectively the d^{th} and $(d, e)^{th}$ entry are given by:

$$\frac{\partial\psi(\mathbf{x}_i, \mathbf{x}_j)}{\partial\mathbf{x}_i^{(d)}} = -\frac{5}{3}\theta^{(d)}\left(\mathbf{x}_i^{(d)} - \mathbf{x}_j^{(d)}\right)\left(1 + \sqrt{5}\mathcal{L}(\mathbf{x}_i, \mathbf{x}_j)\right)\exp\left(-\sqrt{5}\mathcal{L}(\mathbf{x}_i, \mathbf{x}_j)\right) \tag{10}$$

$$\begin{aligned}\frac{\partial^2\psi(\mathbf{x}_i, \mathbf{x}_j)}{\partial\mathbf{x}_i^{(d)}\partial\mathbf{x}_i^{(e)}} = &-\frac{5}{3}\theta^{(d)}\left[\delta_{de}\left(1 + \sqrt{5}\mathcal{L}(\mathbf{x}_i, \mathbf{x}_j)\right) + 5\theta^{(e)}\left(\mathbf{x}_i^{(e)} - \mathbf{x}_j^{(e)}\right)\right.\\ &\left.\cdot\left(\mathbf{x}_i^{(d)} - \mathbf{x}_j^{(d)}\right)\right]\exp\left(-\sqrt{5}\mathcal{L}(\mathbf{x}_i, \mathbf{x}_j)\right)\end{aligned} \tag{11}$$

with δ_{de} the Kronecker delta.

The use of a Gaussian process implies that every prediction corresponds to the assessment of a multivariate normal distribution. This characteristic permits the evaluation of the expected improvement $\mathbb{E}[\mathrm{I}(\mathbf{x})] = EI(\mathbf{x})$ [52] with the improvement of a predicted point on the current best evaluated point, $\mathrm{y}_{min} = \min(\mathrm{y}(\mathbb{X}))$ with $\mathbb{X}$ the set of all samples, defined as (following [35]'s notation): $\mathrm{I}(\mathbf{x}) = (\mathrm{y}_{min} - \mathcal{Y}(\mathbf{x}) \mid \mathrm{Y}(\mathbb{X}) = y(\mathbb{X}))^+$ with $(\cdot)^+ = \max(\cdot, 0)$.

$$\begin{aligned}EI(\mathbf{x}) &= \int_{-\infty}^{\infty}\mathrm{I}(\mathbf{x})\phi(\mathcal{Y}, \mathbf{x})d\mathcal{Y}\\ &= \int_{-\infty}^{\mathrm{y}_{min}}(\mathrm{y}_{min} - \mathcal{Y})\frac{1}{s(\mathbf{x})\sqrt{2\pi}}\exp\left[-\frac{(\mathcal{Y} - \mathrm{Y}(\mathbf{x}))^2}{2s^2(\mathbf{x})}\right]d\mathcal{Y}\end{aligned} \tag{12}$$

which leads to the well-known formula of the expected improvement.

$$EI(\mathbf{x}) = \begin{cases}(\mathrm{y}_{min} - \mathrm{Y}(\mathbf{x}))\Phi\left(u(\mathbf{x})\right) + s(\mathbf{x})\phi\left(u(\mathbf{x})\right) & \text{if } s > 0\\ 0 & \text{otherwise}\end{cases}, \tag{13}$$

with Φ and ϕ respectively the standard normal cumulative and probability density function, ϕ the one-dimensional Gaussian probability density function and $u(\mathbf{x}) = (\mathrm{y}_{min} - \mathrm{Y}(\mathbf{x}))/s(\mathbf{x})$. Note that the first term drives the minimization of the objective (exploitation), while the second term drives the minimization of the uncertainty of the prediction (exploration).

This infill criterion forms the basis of the efficient global optimization (EGO) algorithm by [36] (see Algorithm 1).

Algorithm 1 Efficient Global Optimization (EGO) [36]

Require: Evaluated sampling plan $(\mathbb{X}, \mathrm{y}(\mathbb{X}))$
1: **while** stopping criteria are not met **do**
2: Estimate hyperparameters of Kriging model for objective
3: $\mathbf{x}_{new} = \arg\max_{\mathbf{x}} EI(\mathbf{x})$ ▷ Equation 13
4: $\mathbb{X} \leftarrow \mathbb{X} \cup \mathbf{x}_{new}$
5: $\mathrm{y}_{min} \leftarrow \min_{\mathbf{x}}(\mathrm{y}(\mathbb{X}))$
6: $\mathbf{x}_{min} \leftarrow \arg\min_{\mathbf{x}}(y(\mathbb{X}))$

3 Surrogate-Assisted Asymptotic Reliability Analysis

In this section, an overview of asymptotic reliability-analysis is presented inspired on the work of [41] and extended with an application to Kriging. The aleatory uncertainty corresponds to the noise that corrupts a parameter (Type I) $\boldsymbol{\epsilon}_{\mathbf{u}} \sim \mathcal{N}(\mathbf{0}, \boldsymbol{\Psi}_{\mathbf{u}})$, such that $\mathbf{u} = \mathbf{u} + \boldsymbol{\epsilon}_{\mathbf{u}}$. Design variables are treated as deterministic and in the current section kept constant and omitted from the equations to clarify the equations. They are reintroduced in the following section. We start by reformulating the probability of failure in a Laplace-type integral [9]

$$P_f = \mathbb{P}[g(\mathbf{u}) \leq 0] = \int_{\mathbb{F}} \exp[-\phi(\mathbf{u})] d\mathbf{u} \tag{14}$$

where $\mathbf{u}$ is used to denote a Type I stochastic parameter and $\phi(\mathbf{u}) = -\log(f_{\mathbf{u}}(\mathbf{u}))$ such that ϕ corresponds to the log-likelihood function. The integral can be simplified by approximating the log-likelihood function with a second order Taylor formulation evaluated at $\mathbf{u}^*$, which corresponds to the *most probable failure point* (MPFP)

$$\mathbf{u}^* = \arg \min_{\mathbf{u}} \phi(\mathbf{u}) \quad \text{s.t.} \quad g(\mathbf{u}) \leq 0. \tag{15}$$

The second-order term takes on the form of a Gaussian integral such that the probability of failure reduces to (more details are given in [41, 1]):

$$P_f \approx (2\pi)^{D_{\mathbf{u}}/2} |\mathbf{X}(\mathbf{u}^*)|^{-1/2} \exp(\beta(\mathbf{u}^*)^2/2) \Phi(-\beta(\mathbf{u}^*)) \tag{16}$$

with

$$\mathbf{X}(\mathbf{u})^{(i,j)} = \frac{\partial^2 \phi(\mathbf{u})}{\partial \mathbf{u}^{(i)} \partial \mathbf{u}^{(j)}} + \frac{|\nabla \phi(\mathbf{u})|}{|\nabla g(\mathbf{u})|} \frac{\partial^2 g(\mathbf{u})}{\partial \mathbf{u}^{(i)} \partial \mathbf{u}^{(j)}} \tag{17}$$

$$\sigma(\mathbf{u})^2 = \sum_{i,j=1}^{D_{\mathbf{u}}} \{\mathbf{X}(\mathbf{u})^{-1}\}^{(i,j)} \frac{\partial g(\mathbf{u})}{\partial \mathbf{u}^{(i)}} \frac{\partial g(\mathbf{u})}{\partial \mathbf{u}^{(j)}} \tag{18}$$

$$\beta(\mathbf{u}) = \frac{|\nabla \phi(\mathbf{u})|}{|\nabla g(\mathbf{u})|} \sigma(\mathbf{u}) \tag{19}$$

where $\mathbf{X} \in \mathbb{R}^{D_{\mathbf{u}} \times D_{\mathbf{u}}}$ with $D_{\mathbf{u}}$ the dimensionality of the stochastic variable. With $|\cdot|$ we refer to the L_2-norm in case of a vector and the determinant in case of a matrix. As β goes to infinity, the error in the approximation tends to zero, hence

the name *'asymptotic'*. This formulation can be simplified when $\mathbf{u}$ is defined in a normal space

$$f_{\mathbf{u}}(\mathbf{u})d\mathbf{u} = \frac{1}{(2\pi)^{D_{\mathbf{u}}/2}} \exp\left(-\frac{1}{2}\sum_{d=1}^{D_{\mathbf{u}}}\left(\mathbf{u}^{(d)}\right)^2\right) \tag{20}$$

$$\phi(\mathbf{u}) = \log\left[(2\pi)^{D_{\mathbf{u}}/2}\right] + \frac{1}{2}\sum_{d=1}^{D_{\mathbf{u}}}\left(\mathbf{u}^{(d)}\right)^2 \tag{21}$$

$$\mathbf{X}(\mathbf{u})^{(i,j)} = \delta_{ij} + \sqrt{\sum_{d=1}^{D_{\mathbf{u}}}\left(\mathbf{u}^{(d)}\right)^2}\frac{\partial^2 g(\mathbf{u})}{\partial \mathbf{u}^{(i)}\partial \mathbf{u}^{(j)}}\frac{1}{|\nabla g(\mathbf{u})|} \tag{22}$$

such that

$$P_f \approx \Phi(-\beta(\mathbf{u}^*))|\mathbf{X}(\mathbf{u}^*)|^{-1/2}, \tag{23}$$

with Φ the *standard normal cumulative density function* (CDF). If the curvature of the limit-state surface becomes negligible, β reduces to the distance away from the origin and corresponds to the Hasofer reliability index [31]. Furthermore, $|\mathbf{X}|$ approximates 1 such that we obtain the well-known FORM formulation [41]. If on the other hand the curvature becomes non-negligible, the formulation can still be somewhat simplified through the SORM formalism, which corresponds to the product of FORM with a correction term for curvature, corresponding to the Breitung approximation [8,41]. It can be noted that both are generalizations of the asymptotic reliability analysis described above. However, since gradient and Hessian information is freely available from the surrogate, there is no need for simplifications. The correctness of the assessment of the probability of failure then corresponds to the accuracy of the Taylor approximation of the log-likelihood function and the accuracy of the surrogate model. These concepts are illustrated in Fig. 1 in the bivariate standard normal space.

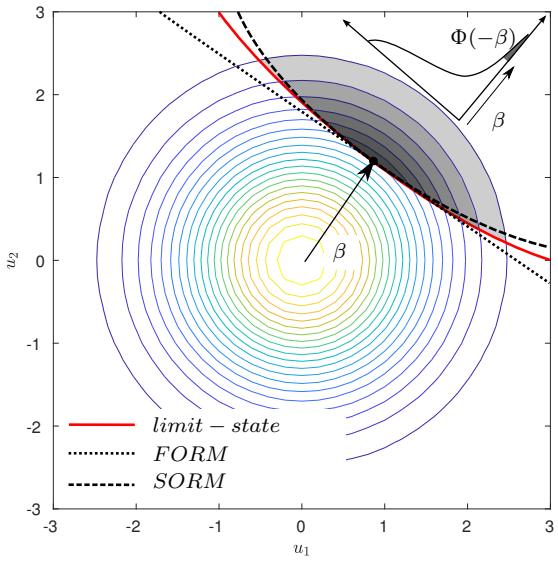

Fig. 1: Contours of the standard normal distribution of the stochastic vector $\mathbf{u}$ and limit-state surface approximations $g(\mathbf{u}) = 0$ ($\beta = |\mathbf{u}^*|$ in case of FORM)

As an example of how the *surrogate-assisted asymptotic reliability analysis* (SARA) will work, we consider a simplified formulation of a limit-state problem of Aoues & Chateauneuf [2]

$$g(\mathrm{x}, \mathrm{u}) = \frac{1}{5}\mathrm{x}^2\mathrm{u}^2 - \mathrm{u} \tag{24}$$

with x a deterministic design variable $0 \leq \mathrm{x} \leq 15$ and u a stochastic parameter (Type I variation) $\mathrm{u} \sim \mathcal{N}(3, 1.5)$. The objective is to determine the probability of failure P_f for every x. To do this, a surrogate of the constraint function is constructed spanning both the deterministic $\mathbb{X}$ and the stochastic space $\mathbb{U}$. For every x, the MPFP is determined (equation 15) to assess the P_f (equation 23). The method is presented in Fig. 2 for a *design of experiments* (DoE) with 17 infills $(11(D_{\mathbf{u}} + D_{\mathbf{x}}) - 5)$ [36].

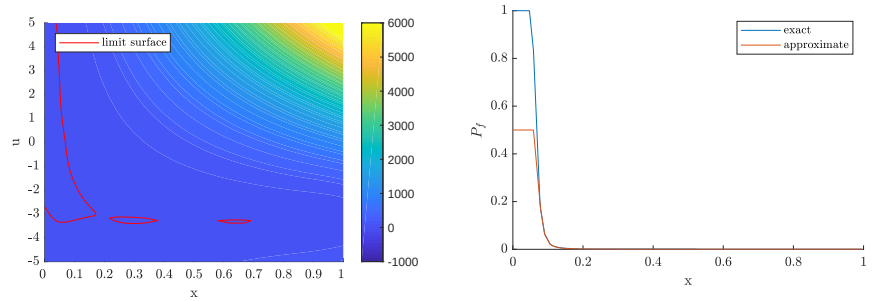

(a) Full factorial assessment of the constraint

(b) P_f(x) using MCS (exact) and SARA (approximate)

Fig. 2: Surrogate-assisted asymptotic reliability analysis (SARA) for test problem Equation 24. x is rescaled to [0,1] and $\mathfrak{u}$ normalized to standard normal. The approximation of P_f is maximum 0.5. However, this is not a problem since we are typically interested in small values.

4 Reliability-Based Design Optimization

The conventional formulation of the *reliability based design optimization* (RBDO) problem typically treats the objective y($\mathbf{x}$) as deterministic or only considers its mean value and presents the probability that the constraints are met as a set of deterministic constraints. This can be formally written as

$$\begin{aligned} \mathbf{x} = &\arg \min_{\mathbf{x}} \ \mathrm{y}(\mathbf{x}) \quad \text{s.t.} \\ &\begin{cases} P_{f,i} = \mathbb{P}[g_i(\mathbf{x},\mathbf{u}) \leq 0] \leq p_{f,i} & i = 1,...,N_{con} \\ d_j\left(\mathbf{x}^{(j)}\right) \leq 0 & j = 1,...,D_{\mathbf{x}} \end{cases} \end{aligned} \tag{25}$$

with $d_j(\mathbf{x}^{(j)})$ the formulation of the design space and N_{con} the number of constraints. Any optimizer (gradient-based such as *sequential quadratic programming* (SQP) or gradient-free such as a *genetic algorithm* (GA)) can be used. The main difficulty is found in the manner by which the constraints are evaluated during the optimization process[6]. Depending on how this is done, Aoues & Chateauneuf divide the different methods that currently exist in literature in three categories: nested, mono-level and decoupled approaches [2,68].

The *nested* or *two-level approach* is characterized by the evaluation of the stochastic constraint in each step of the optimization process. In this category Nikolaidis & Burdisso's *reliability index approach* (RIA) is undoubtedly the most well known [56]. This corresponds to determining the MPFP (equation 15) during each step of the optimization. From the observation that the optimization of a

[6] If a cost can be attributed to the failure of the system, the RBDO problem can be reformulated as a multi-objective optimization problem without constraints. This is typically referred to as *risk optimization* (RO) [5,67].

complex function under a simple constraint is easier than the optimization of a simple function subjected to a complex constraint, Tu et al. presented the *performance measure approach* (PMA) [69,39]. To obtain this, the probability measure is reformulated as a performance measure

$$\beta_f = \Phi^{-1}(1 - \mathbb{P}[g(\mathbf{x}, \mathbf{u}) \leq 0]) \tag{26}$$

by solving an inverse reliability problem, which consists in searching for the point with minimum performance on the target reliability surface, referred to as *minimum performance target point* (MPTP) [2].

$$\mathbf{u}^* = \arg \min_{\mathbf{u}} g(\mathbf{u}) \quad \text{s.t.} \quad |\mathbf{u}| \geq \beta_f \tag{27}$$

The application of surrogate modeling to RBDO is mainly focused to nested approaches: Arsenyev uses a surrogate to perform the optimization and generates for each infill evaluated by the objective function an additional surrogate to determine the probability of failure using his EGOPMA approach [3]. Bichon proposes a single surrogate spanning both deterministic and stochastic spaces where in a nested manner the stochastic space is refined using his EGRA scheme [6] and Dubourg uses the Pollak-He algorithm enhanced with his meta-model-aided importance sampling (Meta-IS) technique to obtain the probability of failure [19, 20].

The *mono-level* (or *single-loop approach*) is used to refer to methods that attempt to avoid the RA altogether by a reformulation of the RBDO problem, such as in Chen et al.'s *single-loop approach* (SLA) [12,38,46], or by replacing the RA by optimality conditions, such as Kuschel & Rackwitz's *Karush-Kuhn-Tucker* (KKT) approach [40]. By doing so, both reliability analysis and design optimization converge in parallel to the optimal solution. However, the authors are not aware of surrogate-aided single-loop approaches.

The *decoupled approaches* are characterized by a decoupling of the reliability analysis and the optimization. According to Aoues & Chateauneuf, one of the most promising methods in this category is the *sequential optimization and reliability assessment* (SORA) by Du & Chen in which the reliability analysis and optimization is reformulated in a cyclic routine [18,76,43]. In each cycle, the reliability assessment is only conducted after the deterministic optimization to verify the constraint on feasibility under uncertainty and this is used to shift the boundaries of violated constraints in the feasible direction in the next cycle. Since it's publication a number of improvements have been proposed: Chen et al. proposed a probabilistic feasible region approach to increase the efficiency [13]. Another promising approach was presented by Cheng et al. with their *sequential approximate programming* (SAP) in which a sequence of sub-programming problems of the approximate problem are solved [14]. A more extensive overview of state-of-the-art RBDO methods is found in [2].

In this work we develop a surrogate-aided single-loop approach relying on the KKT-conditions for both a RIA and PMA formulation of the asymptotic reliability analysis. To fit the problem in a single-loop approach, conform Kuschel & Rackwitz's KKT method, the KKT[7] optimality conditions for both the most probable failure point optimization (equation 15) problem and minimum performance target point optimization (equation 27) are derived.

[7] In the absence of an inequality constraint, the number of KKT conditions reduces to two.

4.1 Single-loop RIA

We define the RIA Lagrangian from the MPFP problem (equation 15): $L_{RIA}(\mathbf{x}, \mathfrak{u}, \mu) = \phi(\mathfrak{u}) + \mu g(\mathbf{x}, \mathfrak{u})$ of which the optimality conditions can be derived:

$$\begin{aligned} KKT_1 &\equiv \mu g(\mathbf{x}, \mathfrak{u}) = 0 \\ KKT_2 &\equiv \nabla_{\mathfrak{u}} L_{RIA}(\mathbf{x}, \mathfrak{u}, \mu) = \nabla_{\mathfrak{u}} \phi(\mathfrak{u}) + \mu \nabla_{\mathfrak{u}} g(\mathbf{x}, \mathfrak{u}) = 0 \end{aligned}$$

Given that $\nabla_{\mathfrak{u}} \phi(\mathfrak{u}) = \mathfrak{u}/|\mathfrak{u}|$, it can be obtained from KKT_2 that $\mathfrak{u} = -\mu|\mathfrak{u}|\nabla_{\mathfrak{u}} g(\mathbf{x}, \mathfrak{u})$ and $|\mathfrak{u}| = \mu|\mathfrak{u}| \cdot |\nabla_{\mathfrak{u}} g(\mathbf{x}, \mathfrak{u})|$ such that the Lagrange multiplier μ can be determined and the conditions can be rewritten as

$$\begin{aligned} KKT_1 &\equiv g(\mathbf{x}, \mathfrak{u}) = 0 \\ KKT_2 &\equiv \mathfrak{u}^T \nabla_{\mathfrak{u}} g(\mathbf{x}, \mathfrak{u}) + |\mathfrak{u}| \cdot |\nabla_{\mathfrak{u}} g(\mathbf{x}, \mathfrak{u})| = 0 \end{aligned}$$

When these conditions are added as constraints to the original RBDO problem (equation 25), the single-loop RIA-based RBDO problem is obtained:

$$\begin{aligned} \mathbf{x} = &\arg \min_{\mathbf{x}} \ \mathrm{y}(\mathbf{x}) \quad \text{s.t.} \\ &\begin{cases} P_{f,i} = \mathbb{P}[g_i(\mathbf{x}, \mathfrak{u}) \leq 0] \leq p_{f,i} & i = 1, ..., N_{con} \\ g_i(\mathbf{x}, \mathfrak{u}) = 0 & i = 1, ..., N_{con} \\ \mathfrak{u}^T \nabla_{\mathfrak{u}} g_i(\mathbf{x}, \mathfrak{u}) + |\mathfrak{u}| \cdot |\nabla_{\mathfrak{u}} g_i(\mathbf{x}, \mathfrak{u})| = 0 & i = 1, ..., N_{con} \\ d_j\left(\mathbf{x}^{(j)}\right) \leq 0 & j = 1, ..., D_{\mathbf{x}} \end{cases} \end{aligned} \tag{28}$$

It can be observed that the constraints of the single-loop RIA-based RBDO can be directly evaluated through the surrogate of the constraint, making it applicability to surrogate-based RBDO especially interesting, notwithstanding the robustness of the optimization problem [69].

4.2 Single-loop PMA

In a similar manner we define the PMA Lagrangian from the MPTP problem (equation 27): $L_{PMA}(\mathfrak{u}, \mu) = g(\mathfrak{u}) + \lambda(|\mathfrak{u}| - \beta_f)$ of which the optimality conditions can be derived:

$$\begin{aligned} KKT_3 &\equiv \lambda(|\mathfrak{u}| - \beta_f) = 0 \\ KKT_4 &\equiv \nabla_{\mathfrak{u}} L_{PMA}(\mathbf{x}, \mathfrak{u}, \lambda) = \nabla_{\mathfrak{u}} g(\mathbf{x}, \mathfrak{u}) + \lambda \nabla_{\mathfrak{u}} |\mathfrak{u}| = 0 \end{aligned}$$

Following a similar approach as in the previous section: the norm of KKT_4 is taken to determine the Lagrangian multiplier λ. As such, we obtain the following equations

$$\begin{aligned} KKT_3 &\equiv |\mathfrak{u}| - \beta_f = 0 \\ KKT_4 &\equiv \mathfrak{u}^T \nabla_{\mathfrak{u}} g(\mathbf{x}, \mathfrak{u}) + |\mathfrak{u}| \cdot |\nabla_{\mathfrak{u}} g(\mathbf{x}, \mathfrak{u})| = 0 \end{aligned}$$

When these conditions are added as constraints to the original RBDO problem (equation 25), the single-loop problem is obtained:

$$\mathbf{x} = \arg\min_{\mathbf{x}} \mathrm{y}(\mathbf{x}) \quad \text{s.t.}$$
$$\begin{cases} P_{f,i} = \mathbb{P}[g_i(\mathbf{x}, \mathbf{u}) \leq 0] \leq p_{f,i} & i = 1, ..., N_{con} \\ |\mathbf{u}| - \beta_{f,i} = 0 & i = 1, ..., N_{con} \\ \mathbf{u}^T \nabla_{\mathrm{u}} g_i(\mathbf{x}, \mathbf{u}) + |\mathbf{u}| \cdot |\nabla_{\mathrm{u}} g_i(\mathbf{x}, \mathbf{u})| = 0 & i = 1, ..., N_{con} \\ d_j \left(\mathbf{x}^{(j)} \right) \leq 0 & j = 1, ..., D_{\mathbf{x}} \end{cases} \tag{29}$$

When fitted in a surrogate-assisted setting where a surrogate is created for the constraint function, the difficulty in performing a single-loop PMA-based RBDO lies in the evaluation of β_f: it can be seen from the approximate formulation of the probability of failure (equation 22 and 23) that β corresponding to a given P_f is a function of the Hessian of g, which is in turn a function of the location in the u-space. Eldred & Bichon propose an iterative approach using Newton's method to obtain β [22]. However, this requires $\nabla_{\mathrm{u}}\beta$ which corresponds to determining the third derivative of the constraint function. In order to ensure continuity of the third derivative of the surrogate, a fitting covariance function must be chosen (for example the exponential covariance function which is infinitely differentiable [60]. However, this might lead to multi-modality of the surrogate of the objective. Alternatively, a quasi-Newton method can be explored, bypassing the third-order derivatives. One can conclude that the reformulation of the PMA-based SARA in a singe-loop introduces a sub-optimization problem, which undermines its initial objective. As such, the method is not explored further here.

5 Efficient Single-Loop Approach

To fit the single-loop RIA methodology in an EGO-like setting, a EI should be defined which fits in this constrained optimization problem. When dealing with a constrained optimization problem, EI should decrease to zero when the constraint is violated. This can be obtained through an extended expected improvement [62] or a penalty function, such as the Augmented Lagrangian function [16]. Here, the former is used: given the surrogate of the constraint $\mathcal{G}$ with $G = \mathbb{E}[\mathcal{G}]$ and $G(\mathbb{X}) = \boldsymbol{g}(\mathbb{X})$, we can calculate the probability of the prediction not violating the constraint limit g_{min}, i.e. the probability that the constraint is met, $P[F(\mathbf{x})]$, where F is the measure of *feasibility* $G(\mathbf{x}) - g_{min}$. Under the assumption of uncorrelated objectives and constraints, it is easy to reformulate the expected improvement such that it accounts for the probability of feasibility $\mathbb{E}[I(\mathbf{x}) \cap F(\mathbf{x})] = \mathbb{E}[I(\mathbf{x})]P[F(\mathbf{x})]$. In case of an inequality constraint, the probability of feasibility corresponds to the cumulative distribution function $P[F(\mathbf{x})] = P[\mathrm{G}(\mathbf{x}) \leq 0] = \Phi(\mathbf{x})$. When dealing with an equality constraint, the difference of two cumulative distribution functions with an offset can be used $P[F(\mathbf{x})] = P[\mathrm{G}(\mathbf{x}) = 0] \approx P[\mathrm{G}(\mathbf{x}) - \epsilon \leq 0 \leq \mathrm{G}(\mathbf{x}) + \epsilon] = \Phi(\mathbf{x} - \boldsymbol{\epsilon}) - \Phi(\mathbf{x} + \boldsymbol{\epsilon})$. This implies that at a given point in the design space, while the predicted constraints might be violated, the predicted errors in the constraint models are different from zero and as such the expectation of feasible improvement will be low, but not zero, since there is a finite possibility that a full evaluation of

the constraints may reveal a feasible design. This allows design space exploration in the early stages of the optimization methodology, but ensures convergence to the exact constrained optimum [23]. Nevertheless, Parr et al. remark that if the constraints are approximated inaccurately early on, the algorithm may discard optimal solutions [57]. Alternatively, Bichon defined the feasibility as [6]:

$$F(\mathbf{x}) \equiv \begin{cases} \epsilon - |\mathrm{G}(\mathbf{x}) - z| & \text{if } z - \epsilon \leq \mathrm{G}(\mathbf{x}) \leq z + \epsilon \\ 0 & \text{elsewhere} \end{cases} \tag{30}$$

from which the *expected feasibility* ($EF = \mathbb{E}[F(\mathbf{x})]$) can be defined

$$\begin{aligned} EF(\mathbf{x}) &= \int_{z-\epsilon}^{z+\epsilon} [\epsilon - |z - \mathcal{G}|] f_{\mathcal{G}} d\mathcal{G} \\ &= (\mathrm{G}(\mathbf{x}) - z) \left[2\Phi^0(\mathbf{x}) - \Phi^{-1}(\mathbf{x}) - \Phi^{+1}(\mathbf{x})\right] + \epsilon \left[\Phi^{+1}(\mathbf{x}) - \Phi^{-1}(\mathbf{x})\right] \\ &\quad + s \left[2\phi^0(\mathbf{x}) - \phi^{-1}(\mathbf{x}) - \phi^{+1}(\mathbf{x})\right] \end{aligned} \tag{31}$$

with

$$\Phi^i(\mathbf{x}) = \Phi\left(\frac{z + i\epsilon - \mathrm{G}(\mathbf{x})}{s(\mathbf{x})}\right), \quad i = -1, 0, +1 \tag{32}$$

$$\phi^i(\mathbf{x}) = \phi\left(\frac{z + i\epsilon - \mathrm{G}(\mathbf{x})}{s(\mathbf{x})}\right), \quad i = -1, 0, +1 \tag{33}$$

The difficulty in the use of EF lies in the choice of ϵ: on the one hand, when chosen too small, the search for feasible points might stagnate. On the other hand, when chosen too big, infeasible points might be selected.

We define the *reliability based expected improvement* (RBEI) as the product of the expected improvement $EI(\mathbf{x})$ with the probability of single-loop reliability $P_{r,sl}(\mathbf{x}, \mathfrak{u})$. The latter corresponds to the product of the probability of feasibility of the probability of failure constraint, $P_r(\mathbf{x}, \mathfrak{u})$, and expected feasibility of the two KKT conditions, $EF[KKT_1(\mathbf{x}, \mathfrak{u})]$ and $EF[KKT_2(\mathbf{x}, \mathfrak{u})]$. With probability of feasibility of the probability of failure the authors refer to the assessment of the correct prediction (an evaluation of the epistemic uncertainty) of the model's prediction of the probability of failure (an evaluation of the aleatoric uncertainty). As such, we obtain

$$RBEI(\mathbf{x}, \mathbf{u}) = EI(\mathbf{x}) \prod_{i=1}^{N_{con}} P_{r,sl,i}(\mathbf{x}, \mathbf{u}) \tag{34}$$

$$P_{r,sl,i}(\mathbf{x}, \mathbf{u}) = P_{r,i}(\mathbf{x}, \mathbf{u}) \cdot EF[KKT_{1,i}(\mathbf{x}, \mathbf{u})] \cdot EF[KKT_{2,i}(\mathbf{x}, \mathbf{u})] \tag{35}$$

with

$$P_{r,i}(\mathbf{x}, \mathbf{u}) = \Phi\left(\frac{p_{f,i} - P_{f,i}(\mathbf{x}, \mathbf{u})}{s_{P_{f,i}}(\mathbf{x}, \mathbf{u})}\right) \tag{36}$$

To evaluate this, the predictive error of the probability of failure (equation 23) s_{P_f} and the second KKT condition s_{KKT_2} must be known. The expected feasibility of the first KKT conditions can be directly evaluated from the surrogate

of the constraint. The MSPE of the second KKT condition can be approximated through a Taylor series based error propagation in which the covariance between the components is omitted. This leads to the following expression

$$s^2_{KKT_2}(\mathbf{x},\mathbf{u}) \approx \sum_{i=1}^{D_\mathbf{u}} \left(\mathbf{u}^{(i)}\right)^2 \cdot s^2_{\partial g/\partial \mathbf{u}^{(i)}}(\mathbf{x},\mathbf{u}) + \left(\sum_{i=1}^{D_\mathbf{u}} \left(\mathbf{u}^{(i)}\right)^2\right) \cdot \left(\sum_{i=1}^{D_\mathbf{u}} s^2_{\partial \mathbf{u}^{(i)}}(\mathbf{x},\mathbf{u})\right) \tag{37}$$

The predictive error of the probability of failure is given by

$$s^2_{P_f}(\mathbf{x},\mathbf{u}) \approx s^2_\Phi(\mathbf{x},\mathbf{u}) \cdot |\mathbf{X}(\mathbf{x},\mathbf{u})|^{-1} + s^2_{|\mathbf{X}|^{-1/2}}(\mathbf{x},\mathbf{u}) \cdot \Phi(\beta(\mathbf{x},\mathbf{u}))^2. \tag{38}$$

To write this as a function of the input is slightly more tedious since the normal cumulative distribution function is a *special function*: it cannot be expressed in terms of elementary functions. Genz & Bretz present a number of approximations [24]. The approximation of the one-dimensional CDF can be obtained through the use of the complementary error function approximation of Karagiannidis & Lioumpas [37]:

$$\begin{aligned}\Phi(\beta(\mathbf{x},\mathbf{u})) &= \frac{1}{2}\left[1 - \operatorname{erfc}\left(\frac{\beta(\mathbf{x},\mathbf{u})}{\sqrt{2}}\right)\right] \\ &\approx \frac{1}{2}\left[1 - \frac{(1-\exp(A\beta(\mathbf{x},\mathbf{u})))\exp(-\beta(\mathbf{x},\mathbf{u})^2/2)}{B\beta(\mathbf{x},\mathbf{u})}\right]\end{aligned} \tag{39}$$

with $A = -1.98/\sqrt{\pi}$ and $B = 1.135\sqrt{\pi/2}$. The predictive error of $\Phi(\beta)$, along with the predictive errors of β (equation 19), $\mathbf{X}$ (equation 22) and σ^2 (equation 18) are respectively given by

$$s^2_{\Phi}(\mathbf{x},\mathbf{u}) = \Big\{(1+\beta(\mathbf{x},\mathbf{u})^4) + \exp(2A\beta(\mathbf{x},\mathbf{u}))(1+A^2\beta(\mathbf{x},\mathbf{u})^2+\beta(\mathbf{x},\mathbf{u})^4) \\ -2\exp\left(A\beta(\mathbf{x},\mathbf{u})\right)\} \cdot \exp\left(-\beta(\mathbf{x},\mathbf{u})^2\right) \cdot B^2 \cdot s^2_{\beta}(\mathbf{x},\mathbf{u}) \tag{40}$$

$$s^2_{\beta}(\mathbf{x},\mathbf{u}) = \sum_{d=1}^{D_{\mathbf{u}}} \left(\mathbf{u}^{(d)}\right)^2 \cdot \left[\frac{s^2_{\sigma}(\mathbf{x},\mathbf{u})}{|\nabla_{\mathbf{u}} g(\mathbf{x},\mathbf{u})|^2} + \sigma^2(\mathbf{x},\mathbf{u}) \cdot s^2_{|\nabla_{\mathbf{u}} g|}(\mathbf{x},\mathbf{u})\right] \tag{41}$$

$$s^2_{|\nabla_{\mathbf{u}} g|}(\mathbf{x},\mathbf{u}) = \frac{\sum_{i=1}^{D_{\mathbf{u}}} \left(\frac{\partial g(\mathbf{x},\mathbf{u})}{\partial \mathbf{u}^{(i)}}\right)^2 \cdot s^2_{\partial g/\partial \mathbf{u}^{(i)}}(\mathbf{x},\mathbf{u})}{\left(\sum_{i=1}^{D_{\mathbf{u}}} \left(\frac{\partial g(\mathbf{x},\mathbf{u})}{\partial \mathbf{u}^{(i)}}\right)^2\right)^2} \tag{42}$$

$$s^2_{\mathbf{X}^{(i,j)}}(\mathbf{x},\mathbf{u}) = \sum_{d=1}^{D_{\mathbf{u}}} \left(\mathbf{u}^{(d)}\right)^2 \cdot \left[\frac{s^2_{\partial^2 g/\partial \mathbf{u}^{(i)}\partial \mathbf{u}^{(i)}}(\mathbf{x},\mathbf{u})}{|\nabla_{\mathbf{u}} g(\mathbf{x},\mathbf{u})|^2} + \left(\frac{\partial^2 g(\mathbf{x},\mathbf{u})}{\partial \mathbf{u}^{(i)}\partial \mathbf{u}^{(j)}}\right)^2 \cdot s^2_{|\nabla_{\mathbf{u}} g|^{-1}}(\mathbf{x},\mathbf{u})\right] \tag{43}$$

$$s^2_{\sigma}(\mathbf{x},\mathbf{u}) = \frac{1}{4\sigma(\mathbf{x},\mathbf{u})^2} \sum_{i,j=1}^{D_{\mathbf{u}}} \Bigg\{ \left[\frac{\partial g(\mathbf{x},\mathbf{u})}{\partial \mathbf{u}^{(i)}} \frac{\partial g(\mathbf{x},\mathbf{u})}{\partial \mathbf{u}^{(j)}}\right]^2 \cdot s^2_{\{\mathbf{X}^{-1}\}^{(i,j)}}(\mathbf{x},\mathbf{u}) \\ + \left[\frac{\partial g(\mathbf{x},\mathbf{u})}{\partial \mathbf{u}^{(i)}} \{\mathbf{X}(\mathbf{x},\mathbf{u})^{-1}\}^{(i,j)}\right]^2 \cdot s^2_{\partial g/\partial \mathbf{u}^{(j)}}(\mathbf{x},\mathbf{u}) \\ + \left[\frac{\partial g(\mathbf{x},\mathbf{u})}{\partial \mathbf{u}^{(j)}} \{\mathbf{X}(\mathbf{x},\mathbf{u})^{-1}\}^{(i,j)}\right]^2 \cdot s^2_{\partial g/\partial \mathbf{u}^{(i)}}(\mathbf{x},\mathbf{u}) \Bigg\} \tag{44}$$

To obtain the predictive error of $\{\mathbf{X}(\mathbf{x},\mathbf{u})^{-1}\}^{(i,j)} = \mathbf{C}(\mathbf{x},\mathbf{u})^{(j,i)}/|\mathbf{X}(\mathbf{x},\mathbf{u})|$, with $\mathbf{C}$ the adjugate matrix, for an arbitrary number of stochastic variables, the predictive error of the determinant must be known. Using Leibniz formula, the determinant of arbitrary dimension can be written as a function of its elements as

$$s^2_{\{\mathbf{X}^{-1}\}^{(i,j)}}(\mathbf{x},\mathbf{u}) = |\mathbf{X}(\mathbf{x},\mathbf{u})|^2 \cdot s^2_{\mathbf{C}^{(j,i)}}(\mathbf{x},\mathbf{u}) + \left(\mathbf{C}^{(j,i)}(\mathbf{x},\mathbf{u})\right)^2 \cdot s^2_{|\mathbf{X}|}(\mathbf{x},\mathbf{u}) \tag{45}$$

$$|\mathbf{X}(\mathbf{x},\mathbf{u})| = \sum_{\sigma \in S_n} \operatorname{sgn}(n) \prod_{i=1}^{n} \mathbf{X}^{(i,\sigma_i)}(\mathbf{x},\mathbf{u}) \tag{46}$$

$$s^2_{|\mathbf{X}|}(\mathbf{x},\mathbf{u}) = \sum_{i,j=1}^{D_{\mathbf{u}}} s^2_{\mathbf{X}^{(i,j)}}(\mathbf{x},\mathbf{u}) \sum_{\sigma \in S_{\mathbb{D}_{\sim i}}} \prod_{k=1}^{D_{\mathbf{u}}-1} \left(\mathbf{X}^{(\{\mathbb{D}_{\sim j}\}_k,\sigma_k)}(\mathbf{x},\mathbf{u})\right)^2 \tag{47}$$

$$s^2_{\mathbf{C}^{(k,l)}}(\mathbf{x},\mathbf{u}) = \sum_{i \in \mathbb{D}_{\sim k}} \sum_{j \in \mathbb{D}_{\sim l}} s^2_{\mathbf{X}^{(i,j)}}(\mathbf{x},\mathbf{u}) \sum_{\sigma \in S_{\mathbb{D}_{\sim ik}}} \prod_{k=1}^{D_{\mathbf{u}}-2} \left(\mathbf{X}^{(\{\mathbb{D}_{\sim jl}\}_k,\sigma_k)}(\mathbf{x},\mathbf{u})\right)^2 \tag{48}$$

with $\mathbb{D} = \{1,...,D_{\mathbf{u}}\}$ and $\mathbb{D}_{\sim i} = \mathbb{D} \backslash i = \{1,...,i-1,i+1,...,D_{\mathbf{u}}\}$.

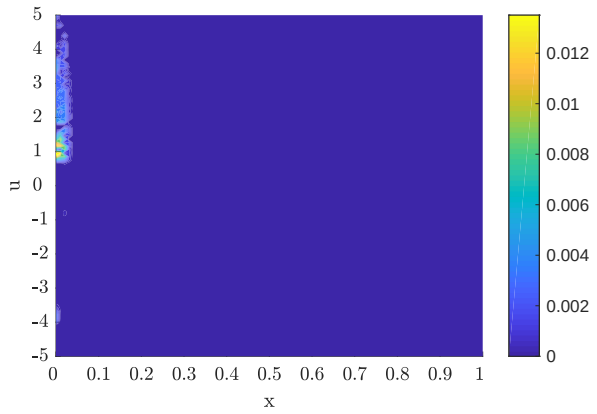

Fig. 3: Reliability-based expected improvement for the RBDO problem in equation 49 after the creation of the surrogates of objective and constraint function using 17 infills (x rescaled to [0,1] and u rescaled/translated to standard normal).

The different components of the RBEI are visualized in Fig. 4 for the simplified RBDO (equation 49).

$$\mathbf{x} = \arg\min_{\mathbf{x}} \quad \mathrm{x}^2 \quad \text{s.t.} \begin{cases} \mathbb{P}\left[\frac{1}{5}\mathrm{x}^2\mathrm{u}^2 - \mathrm{u} \leq 0\right] \leq 0.01 \\ 0 \leq \mathrm{x} \leq 15 \\ \mathrm{u} \sim \mathcal{N}(3, 1.5) \end{cases} \tag{49}$$

The expected improvement (Fig. 4a) is highest for low values of x, independent of u, which is of course to be expected since we are minimizing x^2. P_r (Fig. 4b) is higher away from $\mathrm{u} = 0$, which can again be understood from considering equation 23 and equation 19: with increasing β, P_f decreases. The expected feasibility of the first Karush-Kuhn-Tucker condition takes on a similar form to the limit-state surface, visualized in red in Fig. 2a. Furthermore, it is expected that the expected feasibility of the second Karush-Kuhn-Tucker condition (Fig. 4d) highlights the regions where the MPFP is found. Combining the aforementioned results in the RBEI (Fig. 3) highlighting two interesting regions to be evaluated.

Bringing the aforementioned together allows the formulation of the *Efficient Single-Loop Approach* (ESLA) (see Algorithm 2). First, a sampling plan is constructed containing both deterministic design variables and stochastic parameters. The latter is sampled in the standard[8] normal space. In case of stochastic design variables, they are decomposed as the sum of a deterministic mean and the variation upon the aforementioned: $\mathfrak{x} = \mathbf{x} + \mathbf{u}$ with $\mathbf{u} \sim \mathcal{N}(0, \sigma_{\mathbf{u}})$. This implies that the dimensionality of the problem increases.

[8] Quantities with non-zero mean and a variance that differs from one can be easily rescaled and translated.

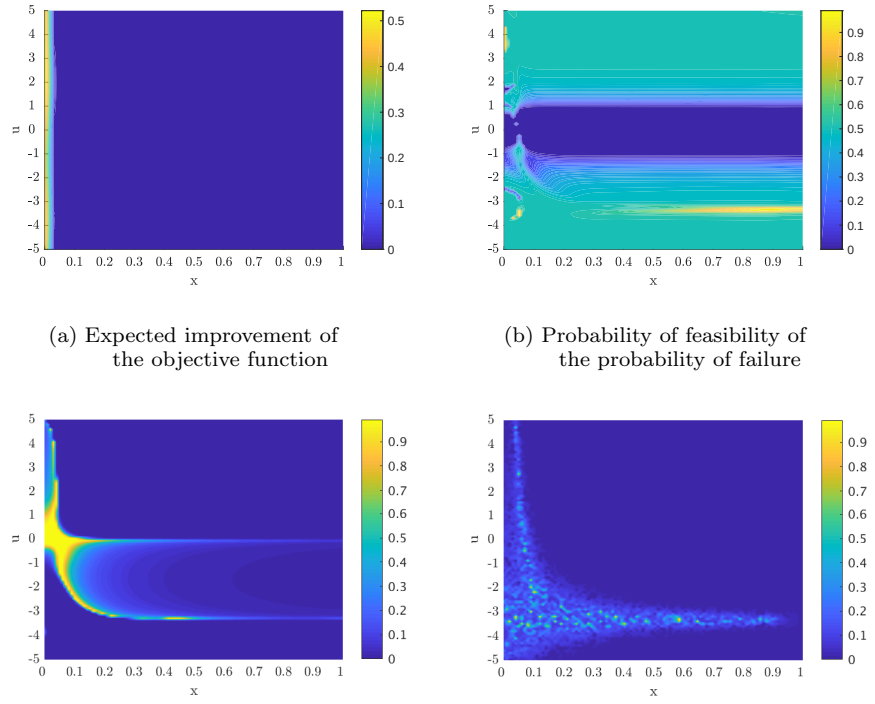

(a) Expected improvement of the objective function

(b) Probability of feasibility of the probability of failure

(c) Expected feasibility of the first Karush-Kuhn-Tucker condition

(d) Expected feasibility of the second Karush-Kuhn-Tucker condition

Fig. 4: Decomposition of the novel infill function for the RBDO problem in equation 49 after the creation of the surrogates of objective and constraint function using 17 infills (x rescaled to [0,1] and $\mathfrak{u}$ rescaled/translated to standard normal).

Following the creating of the surrogates of the objective function and constraints, the probability of failure and KKT conditions of the sampling plan are evaluated. If feasible points exist, the RBEI is calculated upon the best performing point. If not, $P_{r,sl}$ is used as infill function, which is to be maximized. The corresponding point is subsequently evaluated and added to the sampling plan. This process is repeated until a stopping criterion is met.

Finally, the RBDO problem (equation 28) is directly solved on the surrogates using for example SQP or a GA. The best result corresponds with finding an evaluated point. If not, one can still opt to evaluate and validate it. It is important to note at this point that the KKT conditions are only necessary and not sufficient conditions for global optimality in case of non-convex problems. This implies that the optimum obtained by means of a single-loop approach might not correspond to the most severe failure mode [26, 27, 67, 15]. To account for this, one might still opt to solve the RBDO on the surrogate by means of the more conventional RIA- or sampling based approach. However, in case of sampling it is important to

observe that this assumes the availability of an accurate surrogate model. It is to answer this particularity that this novel model acquisition function, the reliability-based expected improvement, is developed. Evaluating the probability of failure by means of sampling using the surrogate implies being subjected to the epistemic uncertainty of the surrogate of the entire domain over which the integration is performed. On the other hand, by basing the acquisition function on the most probable point method, the epistemic uncertainty is reduced to a single point and the uncertainty that comes with the MPP formulation.

Algorithm 2 Efficient Single-Loop Approach (ESLA)

Require: Evaluated sampling plan $(\mathbb{X}, \mathrm{y}(\mathbb{X}))$ and $(\{\mathbb{X}, \mathbb{U}\}, \mathrm{g}(\{\mathbb{X}, \mathbb{U}\}))$
while stopping criteria are not met **do**
  Estimate hyperparameters of Kriging models for objective/constraints ▷ §2
  if Feasible points exist **then**
    $(\mathbf{x}, \mathbf{u})_{new} = \arg\max_{(\mathbf{x},\mathbf{u})} RBEI(\mathbf{x}, \mathbf{u})$ ▷ Equation 34
  else
    $(\mathbf{x}, \mathbf{u})_{new} = \arg\max_{(\mathbf{x},\mathbf{u})} \prod_i P_{r,sl,i}(\mathbf{x}, \mathbf{u})$ ▷ Equation 35
  $\mathrm{y}_{new} = \mathrm{y}(\mathbf{x}_{new})$
  $\mathrm{g}_{new} = \mathrm{g}(\mathbf{x}_{new}, \mathbf{u}_{new})$
  $\mathbb{X} \leftarrow \mathbb{X} \cup \mathbf{x}_{new}$
  $\mathbb{U} \leftarrow \mathbb{U} \cup \mathbf{u}_{new}$
  $\mathrm{y}(\mathbb{X}) \leftarrow \mathrm{y}(\mathbb{X}) \cup \mathrm{y}(\mathbf{x}_{new})$
  $\mathrm{g}(\mathbb{X}, \mathbb{U}) \leftarrow \mathrm{g}(\mathbb{X}, \mathbb{U}) \cup \mathrm{g}(\mathbf{x}_{new}, \mathbf{u}_{new})$
Estimate hyperparameters of Kriging models for objective/constraints ▷ §2
$\mathbf{x} = \arg\min_{\mathbf{x}} \mathrm{y}(\mathbf{x})$ s.t. $P_f \leq p_f$

6 Performance Assessment

The framework is tested on a number of analytical test functions brought forward by Aoues & Chateauneuf that are characterized by difficulties typically encountered in real engineering applications: a nonlinear to highly nonlinear limit-state, multiple limit-states, stochastic design variables and an increasing number of stochastic variables [2]. The latter corresponds to the short column design problem. Furthermore, each test function is examined for 4 levels of reliability.The examples used in the paper lie within the application range of Kriging. Kriging is known to have performance issues when dealing with more than 15 parameters or 500 infills. A unifying overview of methods that attempt to overcome these limitations is amongst other given by Quinonero-Candela and Rasmussen [58].

The first test problem (AC1, Fig. 5) is characterized by a nonlinear limit-state, which makes it especially interesting to examine whether the limit-state approximation is able to find the correct probability of failure.

$$\mathrm{y}(\mathbf{x}) = \left(\mathbf{x}^{(1)}\right)^2 + \left(\mathbf{x}^{(2)}\right)^2 \tag{50}$$

$$g(\mathbf{x}, \mathbf{u}) = \frac{1}{5}\mathbf{x}^{(1)}\mathbf{x}^{(2)}\left(\mathbf{u}^{(2)}\right)^2 - \mathbf{u}^{(1)} \tag{51}$$

with $0 \leq \mathbf{x} \leq 15$, $0 \leq \mathbf{x} \leq 30$, $0 \leq \mathbf{x} \leq 3e2$ and $0 \leq \mathbf{x} \leq 3e4$ for respectively $p_f = 1e{-}2$, $p_f = 1e{-}3$, $p_f = 1e{-}4$ and $p_f = 1e{-}6$. Furthermore, $\mathbf{u}^{(1)} \sim \mathcal{N}(3, 1.5)$ and $\mathbf{u}^{(2)} \sim \mathcal{N}(3, 0.9)$. The optimal solution is respectively given by $\mathbf{x} = [5.65, 5.65]$ with $\mathrm{y}(\mathbf{x}) = 63.85$, $\mathbf{x} = [14.96, 14.96]$ with $\mathrm{y}(\mathbf{x}) = 4.5e2$, $\mathbf{x} = [145.92, 145.92]$ with $\mathrm{y}(\mathbf{x}) = 4.3e4$ and $\mathbf{x} = [9.4e3, 9.4e3]$ with $\mathrm{y}(\mathbf{x}) = 5.3e8$ for $p_f = 1e-2$, $p_f = 1e-3$, $p_f = 1e-4$ and $p_f = 1e-6$.

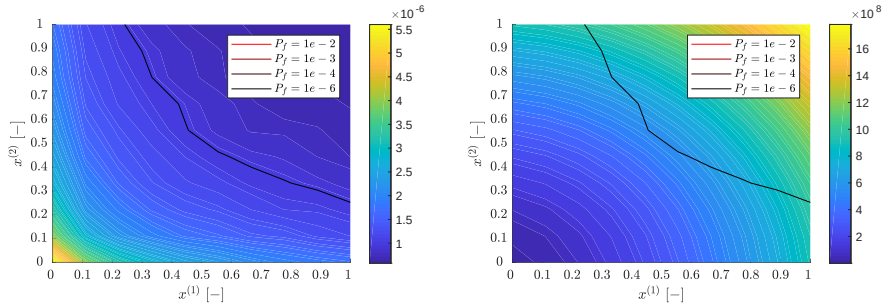

(a) Probability of failure of the constraint

(b) Objective

Fig. 5: Contour plots of AC1 on the normalized design space. The red lines visualize the different limit-state surfaces; darkening with increasing levels of reliability. Note that the lower level reliability limit-surfaces are found in the lower left corner. This is caused by the increase of the size of the design space that was introduced to ensure the existence of a solution to the problems with increasing levels of feasibility.

The second test problem (AC2, Fig. 6) is characterized by an even stronger nonlinear limit-state. Aoues & Chateauneuf used this test function to lay bare the sensitivity to the initial point in case of solving the problem with a gradient-based optimizer. With the problem we intend to illustrate the insensitivity of the scheme to this problem.

$$\mathrm{y}(\mathbf{x}) = \left(\mathbf{x}^{(1)}\right)^2 + \left(\mathbf{x}^{(2)}\right)^2 \tag{52}$$

$$g(\mathbf{x}, \mathbf{u}) = \frac{1}{5}\mathbf{x}^{(1)}\mathbf{x}^{(2)}\left(\mathbf{u}^{(2)}\right)^2 - \log\left(\mathbf{u}^{(1)}\right) \tag{53}$$

with $0 \leq \mathbf{x} \leq 15$, $0 \leq \mathbf{x} \leq 30$, $0 \leq \mathbf{x} \leq 3e2$ and $0 \leq \mathbf{x} \leq 3e4$ for respectively $p_f = 1e{-}2$, $p_f = 1e{-}3$, $p_f = 1e{-}4$ and $p_f = 1e{-}6$. Furthermore, $\mathbf{u}^{(1)} \sim \mathcal{N}(3, 1.5)$ and $\mathbf{u}^{(2)} \sim \mathcal{N}(3, 0.9)$. The optimal solution is respectively given by $\mathbf{x} = [1.35, 1.35]$ with $\mathrm{y}(\mathbf{x}) = 3.65$, $\mathbf{x} = [10.81, 10.81]$ with $\mathrm{y}(\mathbf{x}) = 2.3e2$, $\mathbf{x} = [76.50, 74.34]$ with $\mathrm{y}(\mathbf{x}) = 1.1e3$ and $\mathbf{x} = [1.62e4, 1.62e4]$ with $\mathrm{y}(\mathbf{x}) = 1.8e8$ for $p_f = 1e{-}2$, $p_f = 1e{-}3$, $p_f = 1e-4$ and $p_f = 1e-6$.

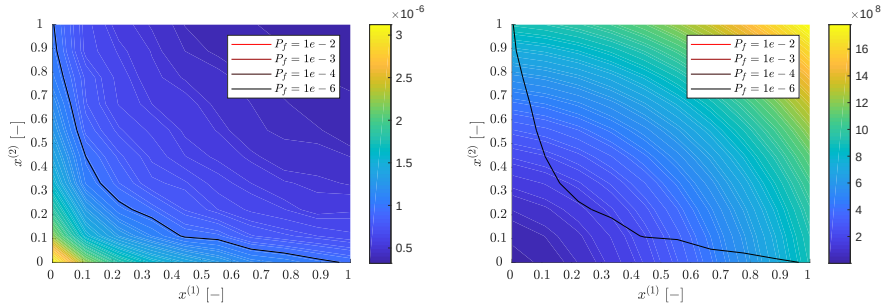

(a) Probability of failure of the constraint (b) Objective

Fig. 6: Contour plots of AC2 on the normalized design space. The red lines visualize the different limit-state surfaces; darkening with increasing levels of reliability. Note that the lower level reliability limit-surfaces are found in the lower left corner. This is caused by the increase of the size of the design space that was introduced to ensure the existence of a solution to the problems with increasing levels of feasibility.

The third test problem (AC3, Fig. 7) is characterized by three different limit-state functions.

$$\mathrm{y}(\mathbf{x}) = \mathbf{x}^{(1)} + \mathbf{x}^{(2)} \tag{54}$$

$$g_1(\mathbf{x}, \mathbf{u}) = \left(\mathbf{u}^{(1)}\right)^2 \mathbf{u}^{(2)}/20 - 1 \tag{55}$$

$$g_2(\mathbf{x}, \mathbf{u}) = \frac{\left(\mathbf{u}^{(1)} + \mathbf{u}^{(2)} - 5\right)^2}{30} + \frac{\left(\mathbf{u}^{(1)} - \mathbf{u}^{(2)} - 12\right)^2}{120} - 1 \tag{56}$$

$$g_3(\mathbf{x}, \mathbf{u}) = \frac{80}{\left(\left(\mathbf{u}^{(1)}\right)^2 + 8\mathbf{u}^{(2)} + 5\right)} - 1 \tag{57}$$

with $0 \leq \mathbf{x} \leq 10$, $\mathbf{u}^{(1)} \sim \mathcal{N}(\mathbf{x}^{(1)}, 0.3)$, $\mathbf{u}^{(2)} \sim \mathcal{N}(\mathbf{x}^{(2)}, 0.3)$ and $p_f = \Phi(-2.0)$, $p_f = \Phi(-3.0)$, $p_f = \Phi(-4.0)$ and $p_f = \Phi(-4.7)$. For which the optimal solution is respectively given by $\mathbf{x} = [3.42, 3.40]$ with $\mathrm{y}(\mathbf{x}) = 6.82$, $\mathbf{x} = [3.61, 3.66]$ with $\mathrm{y}(\mathbf{x}) = 7.27$, $\mathbf{x} = [3.80, 3.80]$ with $\mathrm{y}(\mathbf{x}) = 7.60$ and $\mathbf{x} = [4.00, 4.00]$ with $\mathrm{y}(\mathbf{x}) = 7.92$.

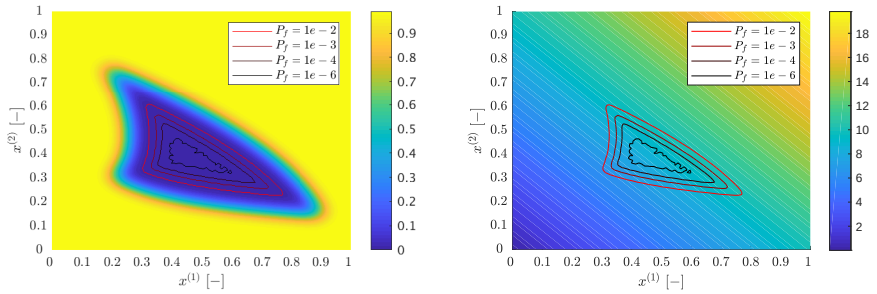

(a) Probability of failure of the constraint (b) Objective

Fig. 7: Contour plots of AC3 on the normalized design space. The red lines visualize the different limit-state surfaces; darkening with increasing levels of reliability.

The forth and final test function (AC4, Fig. 8) corresponds to the short column design problem where we want to minimize the cross section while being subjected to the elastic-plastic constitutive law. The problem is mainly characterized by a higher number of stochastic variables.

$$\mathrm{y}(\mathbf{x}) = \mathbf{x}^{(1)} \cdot \mathbf{x}^{(2)} \tag{58}$$

$$g(\mathbf{x}, \mathbf{u}) = 1 - \frac{4\mathbf{u}^{(2)}}{\mathbf{u}^{(5)} \left(\mathbf{u}^{(6)}\right)^2 \mathbf{u}^{(4)}} - \frac{4\mathbf{u}^{(3)}}{\left(\mathbf{u}^{(5)}\right)^2 \mathbf{u}^{(6)} \mathbf{u}^{(4)}} - \frac{\left(\mathbf{u}^{(1)}\right)^2}{\left(\mathbf{u}^{(4)} \mathbf{u}^{(5)} \mathbf{u}^{(6)}\right)^2} \tag{59}$$

with $0.5 \leq \mathbf{x}^{(1)}/\mathbf{x}^{(2)} \leq 2$, $\mathbf{u}^{(1)} \sim \mathcal{N}(2.5e6, 5e5)$, $\mathbf{u}^{(2)} \sim \mathcal{N}(2.5e5, 7.5e4)$, $\mathbf{u}^{(3)} \sim \mathcal{N}(1.25e5, 3.75e4)$, $\mathbf{u}^{(4)} \sim \mathcal{N}(4e7, 4e6)$, $\mathbf{u}^{(5)} \sim \mathcal{N}(\mathbf{x}^{(1)}, \mathbf{x}^{(1)} \cdot 0.05)$, $\mathbf{u}^{(6)} \sim \mathcal{N}(\mathbf{x}^{(2)}, \mathbf{x}^{(2)} \cdot 0.05)$ and $p_f = \Phi(-2.0)$, $p_f = \Phi(-3.0)$, $p_f = \Phi(-4.0)$ and $p_f = \Phi(-4.7)$. For which the optimal solution is respectively given by $\mathbf{x} = [0.61, 0.31]$ with $\mathrm{y}(\mathbf{x}) = 0.19$, $\mathbf{x} = [0.41, 0.41]$ with $\mathrm{y}(\mathbf{x}) = 0.17$, $\mathbf{x} = [0.48, 0.48]$ with $\mathrm{y}(\mathbf{x}) = 0.23$ and $\mathbf{x} = [0.51, 0.51]$ with $\mathrm{y}(\mathbf{x}) = 0.26$ [77].

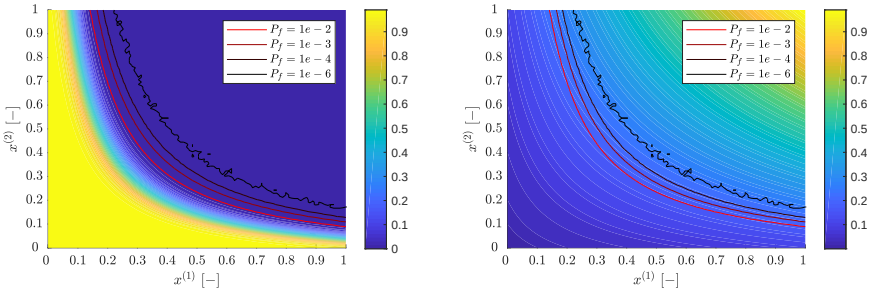

(a) Probability of failure of the constraint

(b) Objective

Fig. 8: Contour plots of AC3 on the normalized design space. The red lines visualize the different limit-state surfaces; darkening with increasing levels of reliability.

For the DoE we use a *Latin Hypercube Sampling* (LHS) approach [51] and Morris & Mitchell's maximin-criterion to quantify the space-filling property by maximizing in ascending order the distance between pairs of points and simultaneously minimizing the number of corresponding pairs [53].

The stopping criteria of the RBDO process corresponds to a maximum of 100 function evaluations after the DoE or if the normalized expected improvement drops below p_f. $11(D_{\mathbf{u}} + D_{\mathbf{x}}) - 5$ infills are initially selected [36]. In RBDO, the objective function is typically treated deterministically, such that the DoE of the objective is much finer. This might lead to a faster decrease of the corresponding MSPE and also an earlier stalling of the convergence because EI might become too small before sufficient accuracy is obtained for the surrogate of the constraint function. The stochastic nature of the optimization caused by the randomly generated DoE can lead to a varying performance. To take this aspect into account,

the optimization is repeated 10 times and the average and standard deviation of the performance metrics are determined. Finding the optimal solution once the stopping criterion is met (Algorithm 2, 14) is performed through SQP using three different formulations: single-loop, RIA and sampling-based. From the perspective that the evaluation of the surrogate is negligible compared to an objective function evaluation (e.g., CFD, CSM or even experiments) this can be justified. However, this does not ensure that the optimal value is obtained. Therefore, the metrics for the assessment of convergence contains both surrogate accuracy and optimizer convergence.

The performance based on the number of limit-state surface evaluations ($f - eval$) is compared with the results published by Aoues & Chateauneuf [2] for the four test functions introduced and two standard representatives of each of the RBDO formulations: Nikolaidus & Burdisso's RIA [56], Tu et al.'s PMA as representatives of the nested formulations [69], Chen et al.'s SLA [12] and Kushel & Rackwitz's KKT [40] as representatives of the single-loop formulation and Du & Chen's SORA [18] and Cheng et al.'s SAP [14] as representatives of the decoupled approaches. Aoues & Chateauneuf use SQP to solve the test problems with a maximum of 100 iterations or a relative change of 10^{-3} as stopping criteria. The HL-RF algorithm is used to solve the MPFP problem in RIA and the HMV algorithm for the MPTP problem in RIA.

Table 1: Number of limit-state evaluations ($f - eval$) till convergence for different methodologies and test functions presented in [2], with NC denoting not converged

	P_f	RIA	PMA	KKT	SLA	SORA	SAP
AC1	1e-2	279/466	189/220	135/211	30/42	138/200	35/48
AC2	1e-2	158/NC	150/210	96/NC	33/60	124/136	72/NC
AC3	$\Phi(-2.0)$	570	612	756	144	348	240
AC4	$\Phi(-3.0)$	604	455	323	43	130	68

Table 2: Performance results of ESLA technique

	P_f	$f-eval$		$\delta_{KKT,x}$		$\delta_{KKT,y}$		$\delta_{RIA,x}$	
		mean	std	mean	std	mean	std	mean	std
AC1	1e-2	136.40	5.0596	0.2711	0.1868	0.0893	0.0635	0.2511	0.1619
	1e-3	138.00	0.0000	0.5651	0.1183	0.2069	0.0769	0.4612	0.0967
	1e-4	64.30	13.3670	0.4341	0.1771	0.1829	0.1009	0.4924	0.2168
	1e-6	44.00	0.0000	0.5316	0.1320	0.2575	0.1186	0.6088	0.1930
AC2	1e-2	138.00	0.0000	0.1972	0.2569	0.0584	0.1358	0.1572	0.0419
	1e-3	123.20	31.2011	0.3932	0.0740	0.1182	0.0207	0.4083	0.1095
	1e-4	64.70	24.9446	0.4035	0.2652	0.2174	0.2121	0.3363	0.1369
	1e-6	87.60	25.3167	0.3219	0.1140	0.0977	0.0005	0.2451	0.1271
AC3	$\Phi(-2.0)$	138.00	0.0000	0.3741	0.1975	0.2078	0.1654	0.4885	0.1337
	$\Phi(-3.0)$	138.00	0.0000	0.5601	0.1332	0.2612	0.0942	0.4440	0.1711
	$\Phi(-4.0)$	138.00	0.0000	0.4291	0.1879	0.1294	0.1255	0.4035	0.1481
	$\Phi(-4.7)$	138.00	0.0000	0.3225	0.1156	0.1192	0.0673	0.4098	0.1715
AC4	$\Phi(-2.0)$	160.00	0.0000	0.1746	0.1056	0.0868	0.0895	0.2833	0.1410
	$\Phi(-3.0)$	160.00	0.0000	0.3344	0.2199	0.1373	0.1639	0.4556	0.1779
	$\Phi(-4.0)$	160.00	0.0000	0.3433	0.2395	0.1973	0.1695	0.3411	0.2065
	$\Phi(-4.7)$	160.00	0.0000	0.2413	0.1937	0.0643	0.0823	0.3760	0.1328

	P_f	$\delta_{RIA,y}$		$\delta_{sampling,x}$		$\delta_{sampling,y}$		$\lvert\partial \mathrm{y} - \partial \mathrm{Y}\rvert$	
		mean	std	mean	std	mean	std	mean	std
AC1	1e-2	0.0818	0.1139	0.1009	0.1862	0.0429	0.1056	0.0072	0.0053
	1e-3	0.1779	0.0672	0.3120	0.1488	0.0836	0.0819	0.0095	0.0092
	1e-4	0.1983	0.1418	0.6675	0.0328	0.2363	0.0036	0.0002	0.0002
	1e-6	0.2572	0.0797	0.4333	0.1326	0.2156	0.0437	0.0118	0.0044
AC2	1e-2	0.0299	0.0139	0.1938	0.0823	0.0469	0.0294	0.0235	0.0289
	1e-3	0.1597	0.1242	0.1602	0.0774	0.0402	0.0239	0.0058	0.0044
	1e-4	0.1181	0.0985	0.3245	0.0604	0.0614	0.0066	0.0007	0.0006
	1e-6	0.0977	0.0006	0.2694	0.1304	0.0977	0.0006	0.0033	0.0017
AC3	$\Phi(-2.0)$	0.3218	0.1220	0.1841	0.1301	0.0664	0.0358	0.0019[a]	0.0018[a]
	$\Phi(-3.0)$	0.2323	0.1745	0.2264	0.1609	0.0696	0.0609	0.0063[a]	0.0045[a]
	$\Phi(-4.0)$	0.1118	0.0971	0.2068	0.0948	0.1029	0.0392	0.0757[a]	0.0450[a]
	$\Phi(-4.7)$	0.1524	0.1509	0.2550	0.1380	0.0900	0.0690	0.1075[a]	0.0684[a]
AC4	$\Phi(-2.0)$	0.1339	0.0803	0.1261	0.0879	0.0384	0.0396	0.0180	0.0113
	$\Phi(-3.0)$	0.1872	0.0993	0.3335	0.1212	0.0801	0.0662	0.0274	0.0123
	$\Phi(-4.0)$	0.1672	0.1667	0.1600	0.1583	0.0460	0.0745	0.0142	0.0102
	$\Phi(-4.7)$	0.2634	0.1510	0.2897	0.2237	0.0969	0.1000	0.0200	0.0165

	P_f	$\lvert\partial^2 \mathrm{y} - \partial^2 \mathrm{Y}\rvert$		$\lvert\partial \mathrm{g}_1 - \partial \mathrm{G}_1\rvert$		$\lvert\partial^2 \mathrm{g}_1 - \partial^2 \mathrm{G}_1\rvert$		$\lvert\partial \mathrm{g}_2 - \partial \mathrm{G}_2\rvert$	
		mean	std	mean	std	mean	std	mean	std
AC1	1e-2	0.0542	0.0306	0.1623	0.0875	0.8640	0.3606	-	-
	1e-3	0.0530	0.0326	1.3404	1.5735	2.1217	1.6844	-	-
	1e-4	0.0435	0.0292	13.996	12.906	5.3607	3.8491	-	-
	1e-6	0.1022	0.0401	397.28	163.19	11.855	3.4305	-	-
AC2	1e-2	0.0812	0.0521	0.3098	0.2149	0.3331	0.1951	-	-
	1e-3	0.0385	0.0269	0.8169	0.5489	2.8227	2.2294	-	-
	1e-4	0.0327	0.0124	40.137	36.393	15.201	12.451	-	-
	1e-6	0.0159	0.0060	189.92	86.5289	6.1918	4.1697	-	-
AC3	$\Phi(-2.0)$	4.1473[a]	0.8013[a]	0.0242	0.0172	0.1109	0.0496	0.0168	0.0195
	$\Phi(-3.0)$	1.4264[a]	0.7613[a]	0.0426	0.0344	0.1139	0.0661	0.0191	0.0116
	$\Phi(-4.0)$	0.7964[a]	0.5770[a]	0.0235	0.0201	0.1056	0.0940	0.0097	0.0083
	$\Phi(-4.7)$	1.2207[a]	0.6758[a]	0.0823	0.0741	0.1699	0.1140	0.0426	0.0271
AC4	$\Phi(-2.0)$	0.1672	0.0830	0.7752	0.6522	3.6791	3.1278	-	-
	$\Phi(-3.0)$	0.2253	0.0889	1.9188	1.4927	3.3500	2.1123	-	-
	$\Phi(-4.0)$	0.1535	0.0569	1.6183	2.8825	3.1673	3.2263	-	-
	$\Phi(-4.7)$	0.1801	0.0898	2.5124	4.2917	5.2436	5.6631	-	-

	P_f	$\lvert\partial^2 \mathrm{g}_2 - \partial^2 \mathrm{G}_2\rvert$		$\lvert\partial \mathrm{g}_3 - \partial \mathrm{G}_3\rvert$		$\lvert\partial^2 \mathrm{g}_3 - \partial^2 \mathrm{G}_3\rvert$	
		mean	std	mean	std	mean	std
AC3	$\Phi(-2.0)$	0.0626	0.0334	0.3970	0.3095	1.8837	1.9450
	$\Phi(-3.0)$	0.0656	0.0191	1.5680	3.3118	6.9730	17.141
	$\Phi(-4.0)$	0.0409	0.0285	0.1124	0.1030	0.5798	0.6247
	$\Phi(-4.7)$	0.0723	0.0307	6.5120	13.139	4.4735	7.9928

[a] Non-normalized since the exact value goes to zero.

The results presented in Table 1 correspond to the number of limit-state surface evaluations ($f - eval$) that are required to converge to the solution. This includes finite difference assessments to obtain the gradients. For the first two test functions and RBDO formulations, two values are presented corresponding to different initial points. NC denotes *Not Converged*. This allows an assessment of robustness of the schemes. The results presented in Table 2 correspond to the performance metrics of ESLA, namely the mean and standard deviation of the number of limit-state surface evaluations ($f - eval$), of the distance in the input and output space between the obtained and exact optimum by means of KKT- ($\delta_{KKT,x}$ and $\delta_{KKT,y}$), RIA- ($\delta_{RIA,x}$ and $\delta_{RIA,y}$) and sampling-based ($\delta_{sampling,x}$ and $\delta_{sampling,y}$) approaches solved using SQP started from a random initial point on the surrogate, and of the norm of the difference between predicted and exact gradient and Hessian in the MPP of the optimum of both the objective ($|\partial \mathrm{y} - \partial \mathrm{Y}|$ and $|\partial^2 \mathrm{y} - \partial^2 \mathrm{Y}|$) and constraint ($|\partial \mathrm{g} - \partial \mathrm{G}|$ and $|\partial^2 \mathrm{g} - \partial^2 \mathrm{G}|$).

In regards to the number of function evaluations ($f - eval$), ESLA proves to be competitive in comparison with state-of-the-art techniques (Table 1); only being outperformed by SLA and SAP in a number of cases. However, this implies little if the accuracy of the surrogate cannot be guaranteed for the stopping criteria defined (maximum 100 infills after the DoE or once the normalized EI becomes smaller than P_f). The accuracy of the surrogates is assessed by examining the norm of the difference between predicted and exact gradient and Hessian in the MPP of the optimum of both the objective and constraint. We can observe that the surrogates obtained by means of the ESLA approach show a consistent accuracy; slightly diminishing with increasing levels of reliability for test problems AC1 and AC2. The latter can be attributed to the lower number of function evaluations, which in turn can be attributed to the formulation of the stopping criteria. A second aspect related to the number of function evaluations is the formulation of the RBEI. Due to the fact that the MSPE of the gradient and Hessian are evaluated, the RBEI does not decrease to zero in evaluated infills. In the worst case, this might lead to a repetitive evaluation of the same infill point or overfitting. To account for this, a penalty function can be superposed on the RBEI.

In regards to the prediction of the optimum on the surrogate by means of KKT-, RIA- and sampling-based approaches using SQP, an expected result is obtained; namely an improving performance when moving from a KKT-, over a RIA-, to a sampling-based setting. However, while one might argue that the computational cost is negligible on the surrogate, an increasing number of samples on the surrogate is required in order to obtain a near-continuous assessment of the probability of failure. With increasing levels of reliability, it can be observed that the performance deteriorates faster than the other methods. This is caused by the fact that 1e6 samples are used for all levels of reliability, which appears to be insufficient in order for SQP to perform well. Making use of more than 1e6 samples makes the method, although surrogate-based, computationally unfeasible. Secondly, SQP, being a local optimizer, will be susceptible to converging to a local optimum, which, in combination with the only necessary conditions of optimality imposed by the KKT conditions, might lead to a local optimum with possibility not the most severe failure mode assessed. To account for the latter, an number of options are available: using alternative formulation of the problem (e.g. SLA, SAP or SORA), making use of a global optimizer (e.g. SQP in a multi-start or

global-search setting or a stochastic optimizer such as GA or ES) or a combination of the two.

In regards to the performace of ESLA with respect to the different aspects of the testfunction, the novel novel scheme proves to be robust. The performance of the scheme does not significantly decrease when comparing test function AC1 and AC2. What is nontheless observable is that the highly non-linear limit-state of the second test function AC2 ($\mathbf{u}^{(1)} \to 0$: $\log(\mathbf{u}^{(1)}) \to \infty$)[9] leads to a larger variance of the number of infills with increasing levels of reliability. This might imply that the MSPEs remain fairly large during the optimization, which in turn indicates that the surrogate has difficulty reproducing the high non-linearity.In case of a multitude of limit-state surfaces (AC3) and a larger number of stochastic parameters (AC4), the schemes does not halt early. This might imply that, independent of the reliability level, 100 infills is insufficient and that the number should be scaled to the dimensionality of the problem and the number of constraints. Nonetheless, ESLA shows a consistent performance in regards to surrogate accuracy based on gradient and Hessian prediction across increasing levels of reliability. This proves the competitiveness of the scheme in comparison with other state-of-the-art methods.

7 Conclusion

In this paper a novel reliability-based design optimization scheme was formulated: the Efficient Single-Loop Approach (ESLA) scheme for Surrogate-Assisted Optimization under Uncertainty (SAOU). The fundamental strengths of the method lie on the one hand in its ability to perform the second-order accurate reliability analysis during each step of the optimization without the need for sampling, assessing gradient and/or Hessian information directly and performing a nested optimization. On the other hand, the efficient approach to finding the most optimal reliable design. The former was obtained by reformulating the problem using the KKT optimality conditions and using surrogates to analytically derive gradient and Hessian information. The latter was obtained by formulating the method as an extension of the Efficient Global Optimization (EGO) scheme through the introduction of a Reliability-Based Expected Improvement (RBEI) that combines the single objective Expected Improvement (EI) with a treatment of the constraints. The result is a surrogate model, accurate in the region of the optimal feasible solution, on which, if needed, an alternative RBDO can be performed without the conventional computational cost. The novel strategy was tested on 4 test functions with 4 levels of reliability characterized by a different set of difficulties encountered in reliability-based design optimization. The results prove the effectiveness of the method to obtain a reliable and optimal solution.

Ongoing research is focused on improving the stopping criteria, such that the method does not halt early. Furthermore, we examine improving the RBEI, such that overfitting or evaluating identical infills is avoided. And finally, we are looking into the most competitive formulation of the RBDO on the surrogate after the final iteration.

[9] At this point, this must be hard coded in the optimization framework that $\mathbf{u}^{(1)}$ may not decrease below zero. The manner by which this is done might also lead to discontinuities in the constraint space and might lead to overfitting.

Appendix: Derivation of the First and Second Derivative of the BLUP and MSPE

The derivation of the *best linear unbiased prediction* (BLUP) and the corresponding *mean square predictive error* (MSPE) are considered as well-known and well-documented and will not be examined here.

For the derivation of the first and second derivatives of the BLUP and their respective MSPEs we make use of a multi-variable formulation of the *difference quotient* (sometimes also referred to as the *Newton's quotient* or *Fermat's quotient*) following McHutchon's approach [50]. Consider the evaluation of the surrogate model at two test point locations

$$\begin{aligned}\mathcal{Y}(\mathbf{x}_*) &= \mathrm{Y}(\mathbf{x}_*) + z_* \\ \mathcal{Y}(\mathbf{x}_* + \boldsymbol{\delta}) &= \mathrm{Y}(\mathbf{x}_* + \boldsymbol{\delta}) + z_\delta\end{aligned}$$

such that (z_*, z_δ) take on the form of a multi-variate Gaussian distribution $P(z_*, z_\delta)$ of which the convariance function is given by

$$\begin{bmatrix} \mathbb{V}[z_*] & \mathbb{C}[z_\delta, z_*] \\ \mathbb{C}[z_*, z_\delta] & \mathbb{V}[z_\delta] \end{bmatrix} \tag{60}$$

and of which the components (with $\mathbb{C}[z_*, z_\delta]$ the covariance) are given by

$$\begin{aligned}\mathbb{C}[z_*, z_\delta] = \sigma^2 \Bigg\{ 1 - \boldsymbol{\psi}(\boldsymbol{x}_*)\boldsymbol{\Psi}^{-1}\boldsymbol{\psi}(\mathbf{x}_* + \boldsymbol{\delta})^T + \Big[\mathbf{F}^T\boldsymbol{\Psi}^{-1}\boldsymbol{\psi}(\mathbf{x}_*) - \boldsymbol{f}(\mathbf{x}_*)\Big]^T \\ \cdot \Big[\mathbf{F}^T\boldsymbol{\Psi}^{-1}\mathbf{F}\Big]^{-1} \cdot \Big[\mathbf{F}^T\boldsymbol{\Psi}^{-1}\boldsymbol{\psi}(\mathbf{x}_* + \boldsymbol{\delta}) - \boldsymbol{f}(\mathbf{x}_* + \boldsymbol{\delta})\Big] \Bigg\}\end{aligned} \tag{61}$$

such that

$$\begin{aligned}\frac{\partial \mathcal{Y}_*}{\partial \mathbf{x}_*} &= \lim_{\boldsymbol{\delta}\to\mathbf{0}} \frac{\mathcal{Y}(\mathbf{x}_* + \boldsymbol{\delta}) - \mathcal{Y}(\mathbf{x}_*)}{\mathbf{x}_* + \boldsymbol{\delta} - \mathbf{x}_*} \\ &= \lim_{\boldsymbol{\delta}\to\mathbf{0}} \frac{\mathrm{Y}(\mathbf{x}_* + \boldsymbol{\delta}) + z_\delta - \mathrm{Y}(\mathbf{x}_* - z_*)}{\boldsymbol{\delta}} \\ &= \lim_{\boldsymbol{\delta}\to\mathbf{0}} \frac{\mathrm{Y}(\mathbf{x}_* + \boldsymbol{\delta}) - \mathrm{Y}(\mathbf{x}_*)}{\boldsymbol{\delta}} + \lim_{\boldsymbol{\delta}\to\mathbf{0}} \frac{z_\delta - z_*}{\boldsymbol{\delta}} \\ &= \frac{\partial \mathrm{Y}_*}{\partial \mathbf{x}_*} + \lim_{\boldsymbol{\delta}\to\mathbf{0}} \frac{z_\delta - z_*}{\boldsymbol{\delta}}\end{aligned}$$

From these results the derivative of the BLUP can be determined.

$$\frac{\partial \mathrm{Y}(\mathbf{x})}{\partial \mathrm{x}_i} = \frac{\partial \boldsymbol{f}(\mathbf{x})}{\partial \mathrm{x}_i}^T \boldsymbol{\beta} + \frac{\partial \boldsymbol{\psi}(\mathbf{x})}{\partial \mathrm{x}_i}^T \boldsymbol{\Psi}^{-1}(\mathbf{y} - \mathbf{F}\boldsymbol{\beta}) \tag{62}$$

In a similar manner, the MSPE of the derivative is derived.

$$
\begin{aligned}
\mathbb{V}\left[\lim_{\boldsymbol{\delta}\to\mathbf{0}}\frac{w_\delta - w_*}{\boldsymbol{\delta}}\right] &= \lim_{\boldsymbol{\delta}\to\mathbf{0}}\frac{1}{\boldsymbol{\delta}^2}\left\{\mathbb{V}[w_\delta] + \mathbb{V}[w_*] - \mathbb{C}[w_\delta, w_*] - \mathbb{C}[w_*, w_\delta]\right\} \\
&= \lim_{\boldsymbol{\delta}\to\mathbf{0}}\frac{\sigma^2}{\boldsymbol{\delta}^2}\Big\{(\boldsymbol{\psi}(\mathbf{x}_* + \boldsymbol{\delta}) - \boldsymbol{\psi}(\mathbf{x}_*))^T\boldsymbol{\Psi}^{-1}((\boldsymbol{\psi}(\mathbf{x}_* + \boldsymbol{\delta}) - \boldsymbol{\psi}(\mathbf{x}_*))) \\
&\quad + \left[\mathbf{F}^T\boldsymbol{\Psi}^{-1}(\boldsymbol{\psi}(\mathbf{x}_* + \boldsymbol{\delta}) - \boldsymbol{\psi}(\mathbf{x}_*)) - (\boldsymbol{f}(\mathbf{x}_* + \boldsymbol{\delta}) - \boldsymbol{f}(\mathbf{x}_*))\right]^T \\
&\quad \cdot \left[\mathbf{F}^T\boldsymbol{\Psi}^{-1}\mathbf{F}\right]^{-1} \cdot \left[\mathbf{F}^T\boldsymbol{\Psi}^{-1} \cdot (\boldsymbol{\psi}(\mathbf{x}_* + \boldsymbol{\delta}) - \boldsymbol{\psi}(\mathbf{x}_*))\right. \\
&\quad \left.-(\boldsymbol{f}(\mathbf{x}_* + \boldsymbol{\delta}) - \boldsymbol{f}(\mathbf{x}_*))\right]\Big\} \\
&= \sigma^2\left\{\frac{\partial\psi}{\partial\mathbf{x}_*}^T\boldsymbol{\Psi}^{-1}\frac{\partial\psi}{\partial\mathbf{x}_*} + \left[\mathbf{F}^T\boldsymbol{\Psi}^{-1}\frac{\partial\psi}{\partial\mathbf{x}_*}^T - \frac{\partial f}{\partial\mathbf{x}_*}\right]^T\right. \\
&\quad \left.\cdot \left[\mathbf{F}^T\boldsymbol{\Psi}^{-1}\mathbf{F}\right]^{-1} \cdot \left[\mathbf{F}^T\boldsymbol{\Psi}^{-1}\frac{\partial\psi}{\partial\mathbf{x}_*}^T - \frac{\partial f}{\partial\mathbf{x}_*}\right]\right\} \qquad (63)
\end{aligned}
$$

The same approach can be repeated to obtain the second derivatives of the BLUP and their respective MSPE.

Conflict of interest

On behalf of all authors, the corresponding author states that there is no conflict of interest.

Replication of Results

The technique was implemented in Matlab by modifying the ooDACE toolbox [17]. Replication of the results can be readily obtained by implementing the SARA and RBEI, and applying them to the test problems.

References

1. Abramowitz, M.: Handbook of Mathematical Functions, With Formulas, Graphs, and Mathematical Tables. Dover Publications, Inc. (1974)
2. Aoues, Y., Chateauneuf, A.: Benchmark study of numerical methods for reliability-based design optimization. Structural and Multidisciplinary Optimization **41**(2), 277–294 (2010). DOI 10.1007/s00158-009-0412-2
3. Arsenyev, I.: Efficient surrogate-based robust design optimization method: Multi-disciplinary design for aero-turbine components. Thesis (2017)
4. Au, S.K., Beck, J.L.: Estimation of small failure probabilities in high dimensions by subset simulation. Probabilistic Engineering Mechanics **16**(4), 263–277 (2001). DOI 10.1016/S0266-8920(01)00019-4
5. Beck, A.T., Gomes, W.J.S., Lopez, R.H., Miguel, L.F.F.: A comparison between robust and risk-based optimization under uncertainty. Structural and Multidisciplinary Optimization **52**(3), 479–492 (2015). DOI 10.1007/s00158-015-1253-9
6. Bichon, B.J.: Efficient surrogate modeling for reliability analysis and design. Thesis (2010)
7. Bichon, B.J., McFarland, J.M., Mahadevan, S.: Efficient surrogate models for reliability analysis of systems with multiple failure modes. Reliability Engineering & System Safety **96**(10), 1386–1395 (2011). DOI 10.1016/j.ress.2011.05.008

8. Breitung, K.: Asymptotic approximations for multinormal integrals. Journal of Engineering Mechanics **110**(3), 357–366 (1984). DOI 10.1061/(ASCE)0733-9399(1984)110:3(357)
9. Breitung, K., Richter, W.D.: A geometric approach to an asymptotic expansion for large-deviation probabilities of gaussian random vectors. Journal of Multivariate Analysis **58**, 1–20 (1996). DOI 10.1006/jmva.1996.0036
10. Bucher, C.: Asymptotic sampling for high-dimensional reliability analysis. Probabilistic Engineering Mechanics **24**(4), 504–510 (2009). DOI 10.1016/j.probengmech.2009.03.002
11. Cao, L., Liu, J., Han, X., Jiang, C., Liu, Q.: An efficient evidence-based reliability analysis method via piecewise hyperplane approximation of limit state function. Structural and Multidisciplinary Optimization **58**(1), 201–213 (2018). DOI 10.1007/s00158-017-1889-8
12. Chen, X., Hasselman, T., Neill, D.: Reliability based structural design optimization for practical applications. Structures, Structural Dynamics, and Materials and Co-located Conferences. American Institute of Aeronautics and Astronautics (1997). DOI 10.2514/6.1997-1403
13. Chen, Z., Li, X., Chen, G., Gao, L., Qiu, H., Wang, S.: A probabilistic feasible region approach for reliability-based design optimization. Structural and Multidisciplinary Optimization **57**(1), 359–372 (2018). DOI 10.1007/s00158-017-1759-4
14. Cheng, G., Xu, L., Jiang, L.: A sequential approximate programming strategy for reliability-based structural optimization. Computers & Structures **84**(21), 1353–1367 (2006). DOI 10.1016/j.compstruc.2006.03.006
15. Chun, J., Paulino, G.H., Song, J.: Reliability-based topology optimization by ground structure method employing a discrete filtering technique. Structural and Multidisciplinary Optimization **60**(3), 1035–1058 (2019). DOI 10.1007/s00158-019-02255-1
16. Conn, A.R., Gould, N.I.M., Toint, P.L.: A Comprehensive Description of the Mathematical Algorithms Used in LANCELOT, pp. 102–132. Springer Berlin Heidelberg, Berlin, Heidelberg (1992). DOI 10.1007/978-3-662-12211-2_3
17. Couckuyt, I., Dhaene, T., Demeester, P.: ooDACE toolbox: a flexible object-oriented kriging implementation. J. Mach. Learn. Res. **15**(1), 3183–3186 (2014)
18. Du, X., Chen, W.: Sequential optimization and reliability assessment method for efficient probabilistic design. Journal of Mechanical Design **126**(2), 225–233 (2004). DOI 10.1115/1.1649968
19. Dubourg, V.: Adaptive surrogate models for reliability analysis and reliability-based design optimization. Thesis (2011)
20. Dubourg, V., Sudret, B.: Meta-model-based importance sampling for reliability sensitivity analysis. Structural Safety **49**, 27–36 (2014). DOI 10.1016/j.strusafe.2013.08.010
21. Echard, B., Gayton, N., Lemaire, M., Relun, N.: A combined importance sampling and kriging reliability method for small failure probabilities with time-demanding numerical models. Reliability Engineering & System Safety **111**, 232–240 (2013). DOI 10.1016/j.ress.2012.10.008
22. Eldred, M., Bichon, B.: Second-Order Reliability Formulations in DAKOTA/UQ. Structures, Structural Dynamics, and Materials and Co-located Conferences. American Institute of Aeronautics and Astronautics (2006). DOI 10.2514/6.2006-1828
23. Forrester, A., Sóbester, A., Keane, A.: Engineering Design via Surrogate Modelling: A Practical Guide. Wiley (2008)
24. Genz, A., Bretz, F.: Computation of Multivariate Normal and t Probabilities, *Lecture Notes in Statistics*, vol. 195. Springer-Verlag Berlin Heidelberg (2009). DOI 10.1007/978-3-642-01689-9
25. Grooteman, F.: Adaptive radial-based importance sampling method for structural reliability. Structural Safety **30**(6), 533–542 (2008). DOI 10.1016/j.strusafe.2007.10.002
26. Guo, X., Bai, W., Zhang, W., Gao, X.: Confidence structural robust design and optimization under stiffness and load uncertainties. Computer Methods in Applied Mechanics and Engineering **198**(41), 3378–3399 (2009). DOI 10.1016/j.cma.2009.06.018
27. Guo, X., Du, J., Gao, X.: Confidence structural robust optimization by non-linear semidefinite programming-based single-level formulation. International Journal for Numerical Methods in Engineering **86**(8), 953–974 (2011). DOI 10.1002/nme.3083
28. Haldar, A., Mahadevan, S.: Probability, Reliability, and Statistical Methods in Engineering Design. Wiley: New York (2000)
29. Han, Z.H., Görtz, S., Zimmermann, R.: Improving variable-fidelity surrogate modeling via gradient-enhanced kriging and a generalized hybrid bridge function. Aerospace Science and Technology **25**(1), 177–189 (2013). DOI 10.1016/j.ast.2012.01.006

30. Han, Z.H., Zhang, Y., Song, C.X., Zhang, K.S.: Weighted gradient-enhanced kriging for high-dimensional surrogate modeling and design optimization. AIAA Journal **55**(12), 4330–4346 (2017). DOI 10.2514/1.J055842
31. Hasofer, A.M., Lind, N.C.: Exact and invariant second moment code. Journal of the Engineering Mechanics Division **100**(1), 111–121 (1974)
32. Hawchar, L., El Soueidy, C.P., Schoefs, F.: Global kriging surrogate modeling for general time-variant reliability-based design optimization problems. Structural and Multidisciplinary Optimization **58**(3), 955–968 (2018). DOI 10.1007/s00158-018-1938-y
33. Hu, Z., Mahadevan, S.: Global sensitivity analysis-enhanced surrogate (gsas) modeling for reliability analysis. Structural and Multidisciplinary Optimization **53**(3), 501–521 (2016). DOI 10.1007/s00158-015-1347-4
34. Huang, Z.L., Jiang, C., Zhang, Z., Zhang, W., Yang, T.G.: Evidence-theory-based reliability design optimization with parametric correlations. Structural and Multidisciplinary Optimization **60**(2), 565–580 (2019). DOI 10.1007/s00158-019-02225-7
35. Janusevskis, J., Le Riche, R., Ginsbourger, D., Girdziusas, R.: Expected improvements for the asynchronous parallel global optimization of expensive functions: Potentials and challenges. In: Y. Hamadi, M. Schoenauer (eds.) Learning and Intelligent Optimization, pp. 413–418. Springer Berlin Heidelberg (2012)
36. Jones, D.R., Schonlau, M., Welch, W.J.: Efficient global optimization of expensive black-box functions. Journal of Global Optimization **13**(4), 455–492 (1998). DOI 10.1023/A:1008306431147
37. Karagiannidis, G.K., Lioumpas, A.S.: An improved approximation for the gaussian q-function. IEEE Communications Letters **11**(8), 644–646 (2007). DOI 10.1109/LCOMM.2007.070470
38. Keshtegar, B., Hao, P.: Enhanced single-loop method for efficient reliability-based design optimization with complex constraints. Structural and Multidisciplinary Optimization **57**(4), 1731–1747 (2018). DOI 10.1007/s00158-017-1842-x
39. Keshtegar, B., Lee, I.: Relaxed performance measure approach for reliability-based design optimization. Structural and Multidisciplinary Optimization **54**(6), 1439–1454 (2016). DOI 10.1007/s00158-016-1561-8
40. Kuschel, N., Rackwitz, R.: Two basic problems in reliability-based structural optimization. Mathematical Methods of Operations Research **46**(3), 309–333 (1997). DOI 10.1007/BF01194859
41. Langley, R.S.: Unified approach to probabilistic and possibilistic analysis of uncertain systems. Journal of Engineering Mechanics **126**(11), 1163–1172 (2000). DOI 10.1061/(ASCE)0733-9399(2000)126:11(1163)
42. Lemaire, M., Chateauneuf, A., Mitteau, J.C.: Structural Reliability. Wiley-ISTE (2009)
43. Li, F., Liu, J., Wen, G., Rong, J.: Extending sora method for reliability-based design optimization using probability and convex set mixed models. Structural and Multidisciplinary Optimization **59**(4), 1163–1179 (2019). DOI 10.1007/s00158-018-2120-2
44. Li, H.S., Cao, Z.J.: Matlab codes of subset simulation for reliability analysis and structural optimization. Structural and Multidisciplinary Optimization **54**(2), 391–410 (2016). DOI 10.1007/s00158-016-1414-5
45. Li, M., Bai, G., Wang, Z.: Time-variant reliability-based design optimization using sequential kriging modeling. Structural and Multidisciplinary Optimization **58**(3), 1051–1065 (2018). DOI 10.1007/s00158-018-1951-1
46. Li, X., Meng, Z., Chen, G., Yang, D.: A hybrid self-adjusted single-loop approach for reliability-based design optimization. Structural and Multidisciplinary Optimization **60**(5), 1867–1885 (2019). DOI 10.1007/s00158-019-02291-x
47. Ling, C., Lu, Z., Feng, K., Sun, B.: Efficient numerical simulation methods for estimating fuzzy failure probability based importance measure indices. Structural and Multidisciplinary Optimization **59**(2), 577–593 (2019). DOI 10.1007/s00158-018-2085-1
48. Ling, C., Lu, Z., Feng, K., Zhang, X.: A coupled subset simulation and active learning kriging reliability analysis method for rare failure events. Structural and Multidisciplinary Optimization **60**(6), 2325–2341 (2019). DOI 10.1007/s00158-019-02326-3
49. Liu, X., Wang, X., Xie, J., Li, B.: Construction of probability box model based on maximum entropy principle and corresponding hybrid reliability analysis approach. Structural and Multidisciplinary Optimization **61**(2), 599–617 (2020). DOI 10.1007/s00158-019-02382-9
50. McHutchon, A.: Differentiating Gaussian processes (2013). URL http://mlg.eng.cam.ac.uk/mchutchon/DifferentiatingGPs.pdf

51. McKay, M.D., Beckman, R.J., Conover, W.J.: A comparison of three methods for selecting values of input variables in the analysis of output from a computer code. Technometrics **21**(2), 239–245 (1979). DOI 10.2307/1268522
52. Mockus, J., Tiesis, V., Zilinskas, A.: The application of bayesian methods for seeking the extremum. In: L.D. 2, G. Szego (eds.) Towards Global Optimization 2: Proceedings of a Workshop at the University of Cagliari, Italy, October 1974, vol. 2, pp. 117–129 (1978)
53. Morris, M.D., Mitchell, T.J.: Exploratory designs for computational experiments. Journal of Statistical Planning and Inference **43**(3), 381–402 (1995). DOI 10.1016/0378-3758(94)00035-T
54. Moustapha, M., Sudret, B.: Surrogate-assisted reliability-based design optimization: a survey and a unified modular framework. Structural and Multidisciplinary Optimization **60**(5), 2157–2176 (2019). DOI 10.1007/s00158-019-02290-y
55. Naess, A., Leira, B.J., Batsevych, O.: System reliability analysis by enhanced monte carlo simulation. Structural Safety **31**(5), 349–355 (2009). DOI https://doi.org/10.1016/j.strusafe.2009.02.004
56. Nikolaidis, E., Burdisso, R.: Reliability based optimization: A safety index approach. Computers & Structures **28**(6), 781–788 (1988). DOI https://doi.org/10.1016/0045-7949(88)90418-X
57. Parr, J.M., Keane, A.J., Forrester, A.I.J., Holden, C.M.E.: Infill sampling criteria for surrogate-based optimization with constraint handling. Engineering Optimization **44**(10), 1147–1166 (2012). DOI 10.1080/0305215X.2011.637556
58. Quinonero-Candela, J., Rasmussen, C.E.: A unifying view of sparse approximate gaussian process regression. Journal of Machine Learning Research **6**, 1939–1959 (2005)
59. Rackwitz, R.: Reliability analysis-a review and some perspectives. Structural Safety **23**, 365–395 (2001). DOI 10.1016/S0167-4730(02)00009-7
60. Rasmussen, C.E., Williams, C.K.I.: Gaussian Processes for Machine Learning. the MIT Press (2006)
61. Rubinstein, R.Y., Kroese, D.P.: Simulation and the Monte Carlo Method. Wiley Series in Probability and Statistics. John Wiley & Sons, Inc (2016). DOI 10.1002/9781118631980
62. Schonlau, M., Welch, W.J., Jones, D.R.: Global versus local search in constrained optimization of computer models, *Lecture Notes–Monograph Series*, vol. Volume 34, pp. 11–25. Institute of Mathematical Statistics, Hayward, CA (1998). DOI 10.1214/lnms/1215456182
63. Shi, Y., Lu, Z., Xu, L., Zhou, Y.: Novel decoupling method for time-dependent reliability-based design optimization. Structural and Multidisciplinary Optimization **61**(2), 507–524 (2020). DOI 10.1007/s00158-019-02371-y
64. Sichani, M.T., Nielsen, S.R.K., Bucher, C.: Efficient estimation of first passage probability of high-dimensional nonlinear systems. Probabilistic Engineering Mechanics **26**(4), 539–549 (2011). DOI 10.1016/j.probengmech.2011.05.013
65. Stein, M.L.: A kernel approximation to the kriging predictor of a spatial process. Annals of the Institute of Statistical Mathematics **43**(1), 61–75 (1991). DOI 10.1007/BF00116469
66. Sudret, B.: Meta-models for structural relibiality and uncertainty quantification. In: K.K. Phoon, M. Beer, S.T. Quek, S.D. Pang (eds.) Fifth Asian-Pacific Symposium on Structural Reliability and its Applications (5APSSRA) (2012). DOI 10.3850/981-973-0000-00-0_SudretKeynote
67. Torii, A.J., Lopez, R.H., Beck, A.T., Miguel, L.F.F.: A performance measure approach for risk optimization. Structural and Multidisciplinary Optimization **60**(3), 927–947 (2019). DOI 10.1007/s00158-019-02243-5
68. Torii, A.J., Lopez, R.H., F. Miguel, L.F.: A general rbdo decoupling approach for different reliability analysis methods. Structural and Multidisciplinary Optimization **54**(2), 317–332 (2016). DOI 10.1007/s00158-016-1408-3
69. Tu, J., Choi, K.K., Park, Y.H.: A new study on reliability-based design optimization. Journal of Mechanical Design **121**(4), 557–564 (1999). DOI 10.1115/1.2829499
70. Wang, D., Jiang, C., Qiu, H., Zhang, J., Gao, L.: Time-dependent reliability analysis through projection outline-based adaptive kriging. Structural and Multidisciplinary Optimization **61**(4), 1453–1472 (2020). DOI 10.1007/s00158-019-02426-0
71. Wang, L., Liang, J., Wu, D.: A non-probabilistic reliability-based topology optimization (nrbto) method of continuum structures with convex uncertainties. Structural and Multidisciplinary Optimization **58**(6), 2601–2620 (2018). DOI 10.1007/s00158-018-2040-1
72. Wei, P., Wang, Y., Tang, C.: Time-variant global reliability sensitivity analysis of structures with both input random variables and stochastic processes. Structural and Multidisciplinary Optimization **55**(5), 1883–1898 (2017). DOI 10.1007/s00158-016-1598-8

73. Xie, S., Pan, B., Du, X.: High dimensional model representation for hybrid reliability analysis with dependent interval variables constrained within ellipsoids. Structural and Multidisciplinary Optimization **56**(6), 1493–1505 (2017). DOI 10.1007/s00158-017-1806-1
74. Yang, X., Liu, Y., Fang, X., Mi, C.: Estimation of low failure probability based on active learning kriging model with a concentric ring approaching strategy. Structural and Multidisciplinary Optimization **58**(3), 1175–1186 (2018). DOI 10.1007/s00158-018-1960-0
75. Yao, W., Tang, G., Wang, N., Chen, X.: An improved reliability analysis approach based on combined form and beta-spherical importance sampling in critical region. Structural and Multidisciplinary Optimization **60**(1), 35–58 (2019). DOI 10.1007/s00158-019-02193-y
76. Yi, P., Zhu, Z., Gong, J.: An approximate sequential optimization and reliability assessment method for reliability-based design optimization. Structural and Multidisciplinary Optimization **54**(6), 1367–1378 (2016). DOI 10.1007/s00158-016-1478-2
77. Youn, B.D., Choi, K.K.: An investigation of nonlinearity of reliability-based design optimization approaches. Journal of Mechanical Design **126**(3), 403–411 (2003). DOI 10.1115/1.1701880
78. Yun, W., Lu, Z., Jiang, X.: An efficient reliability analysis method combining adaptive kriging and modified importance sampling for small failure probability. Structural and Multidisciplinary Optimization **58**(4), 1383–1393 (2018). DOI 10.1007/s00158-018-1975-6
79. Yun, W., Lu, Z., Zhou, Y., Jiang, X.: Ak-sysi: an improved adaptive kriging model for system reliability analysis with multiple failure modes by a refined u learning function. Structural and Multidisciplinary Optimization **59**(1), 263–278 (2019). DOI 10.1007/s00158-018-2067-3
80. Zang, T.A., Hemsch Michael, J., Hilburger, M.W., Kenny, S.P., Luckring, J.M., Peiman, M., Padula, S.L., Stroud, W.J.: Needs and opportunities for uncertainty-based multidisciplinary design methods for aerospace vehicles. Report TM-2002-211462, NASA (2002)
81. Zhang, Z., Jiang, C., Ruan, X.X., Guan, F.J.: A novel evidence theory model dealing with correlated variables and the corresponding structural reliability analysis method. Structural and Multidisciplinary Optimization **57**(4), 1749–1764 (2018). DOI 10.1007/s00158-017-1843-9
82. Zheng, J., Luo, Z., Jiang, C., Ni, B., Wu, J.: Non-probabilistic reliability-based topology optimization with multidimensional parallelepiped convex model. Structural and Multidisciplinary Optimization **57**(6), 2205–2221 (2018). DOI 10.1007/s00158-017-1851-9